Automatic Liver Tumor Segmentation in Computed Tomography (CT) Imaging

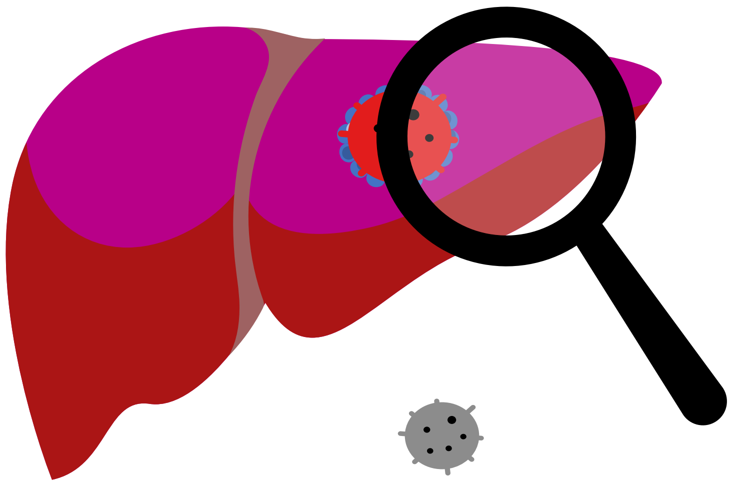

Thesis Final Exam

Name: Kasun Gayashan Hettihewa
Student ID: 6470369721

4th December 2023

Advisor: Assoc. Prof. Thanarat Chalidabhongse, Ph.D

Table of contents

01 Introduction

Introduction: Background

Liver Tumors

- Malignant (Cancerous)
  - Primary
    - Hepatocellular carcinoma (HCC)
    - Intrahepatic cholangiocarcinoma (ICC)
    - Angiosarcoma and hemangiosarcoma
    - Hepatoblastoma
  - Secondary (metastatic liver cancer)
- Benign (Not Cancerous)
  - Hemangioma
  - Hepatic adenoma
  - Focal nodular hyperplasia (FNH)

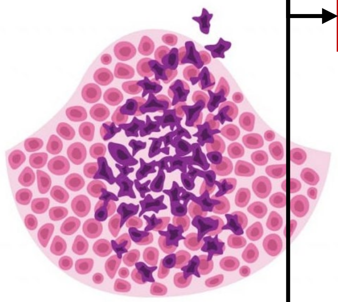

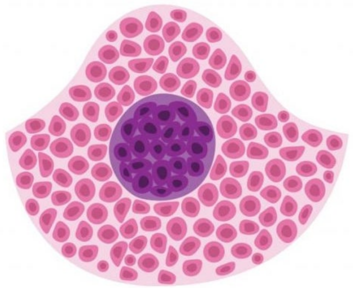

[1]https://www.cancer.org/cancer/liver-cancer/about/what-is-liver-cancer.html

Introduction: Background

Computer-Aided Diagnosis (CAD) System and CT imaging

CAD is a computer-integrated technology that **supports clinical decision making for radiologists** by providing **automatic medical image analysis** using computer algorithms.

CT is radiological imaging that visualizes the liver. Radiologists examine the CT images manually based on their experience to recognize abnormalities in the liver that can be cancerous.

Introduction: Clinical challenges

- Same type of tumors can show different growth patterns[1]
- Same type of tumors can change the appearance based on the location of the liver[1]
- Diseased liver can hinder the recognition of tumors in earlier stages (Ex: Cirrhosis)[1]
- Identification of the tumor stage for treatment planning[2]
- Tumor diameter measurement for treatment planning[2]
- Tumor localization for treatment planning[2]

[1]Quaglia A. Hepatocellular carcinoma: a review of diagnostic challenges for the pathologist. *J Hepatocell Carcinoma*. 2018;5:99-108. https://doi.org/10.2147/JHC.S15980

[2]Bilic, P. et al. The liver tumor segmentation benchmark (LiTS). Med. Image Anal. 84, 102680. https://doi.org/10.1016/j.media.2022.102680 (2023).

Introduction: Technical challenges

Variability in size, shape and intensity values.

Variations in contrast enhancement

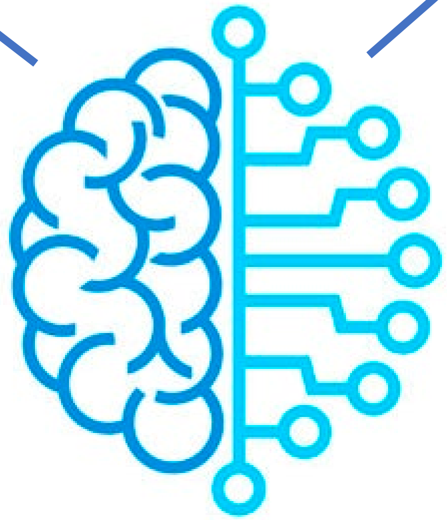

Disease-specific variability

Lack of radiological data

Multiple tumors with variable texture patterns

[1]Bilic, P. et al. The liver tumor segmentation benchmark (LiTS). Med. Image Anal. 84, 102680. https://doi.org/10.1016/j.media.2022.102680 (2023).

Objectives

To develop a Computer-Aided Diagnosis (CAD) tool to segment liver tumors from computed tomography (CT) imaging by utilizing less computational cost. Assess and validate the applicability of the development with a radiologist.

Scope

01

The proposed model can correctly segment liver tumors compared to baseline method.

02

The proposed model utilizes less computational cost compared to baseline method.

03

The study is conducted with scans only with liver tumors.

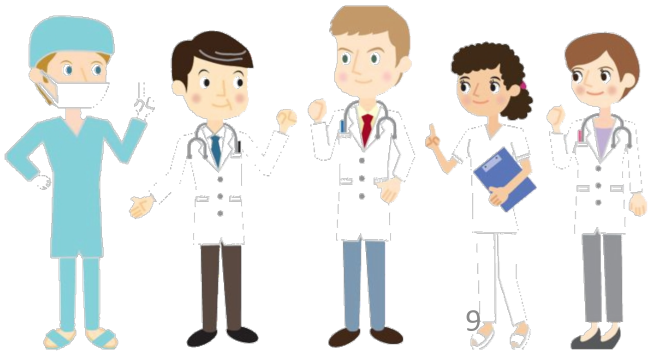

02

Literature Survey

Literature Surveys

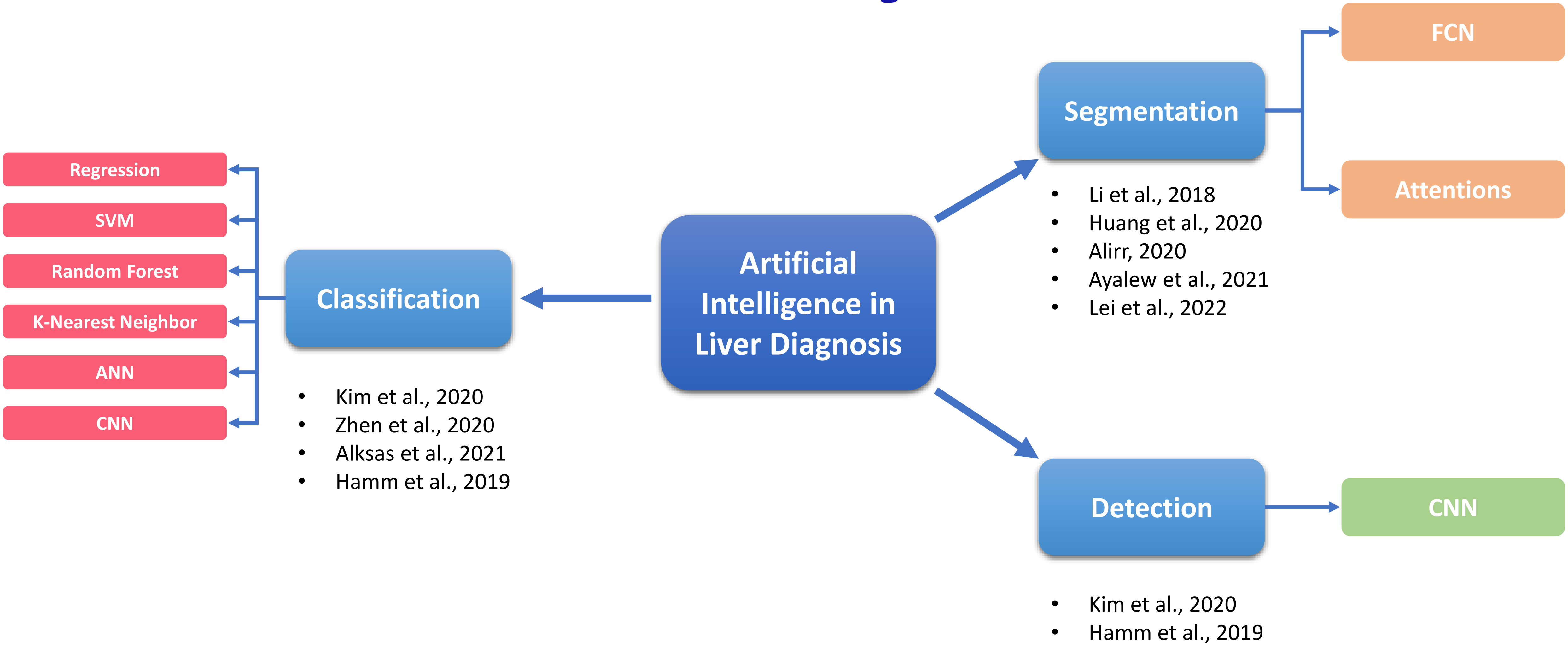

Literature Surveys

Segmentation

FCN

- FCN (Long et al., 2015)
- UNet (Ronneberger et al., 2015)
- H-DenseUnet (Li et al., 2018)
- U-Net++ (Zhou et al., 2018)
- ResUNet (Zhang et al., 2018)
- UNet 3+ (Huang et al., 2020)

Attentions

- Attention U-Net (Oktay et al., 2018)
- ResUNet++ (Zhang et al., 2018)
- Squeeze-and-excitation (Hu et al., 2018)
- MS-UNet (Kushnure and Talbar, 2021)
- HFRU-Net (Kushnure and Talbar, 2022)
- CBAM (Woo et al., 2018)
- S-Net (Luan et al., 2021)
- TA-Net (Pang et al., 2021)
- SmaAt-UNet (Trebing et al., 2021)

Literature Surveys

Segmentation

FCN

- FCN (Long et al., 2015)
- UNet (Ronneberger et al., 2015)
- H-DenseUnet (Li et al., 2018)
- U-Net++ (Zhou et al., 2018)
- ResUNet (Zhang et al., 2018)
- UNet 3+ (Huang et al., 2020)

Attentions

- Attention U-Net (Oktay et al., 2018)
- ResUNet++ (Zhang et al., 2018)
- Squeeze-and-excitation (Hu et al., 2018)
- MS-UNet (Kushnure and Talbar, 2021)
- HFRU-Net (Kushnure and Talbar, 2022)
- CBAM (Woo et al., 2018)
- S-Net (Luan et al., 2021)
- TA-Net (Pang et al., 2021)
- SmaAt-UNet (Trebing et al., 2021)

03 Proposed Method

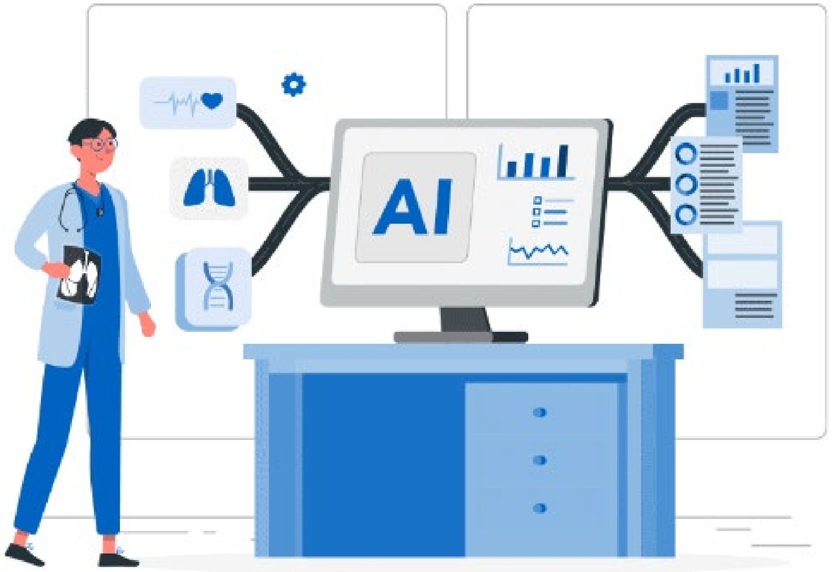

Proposed Method

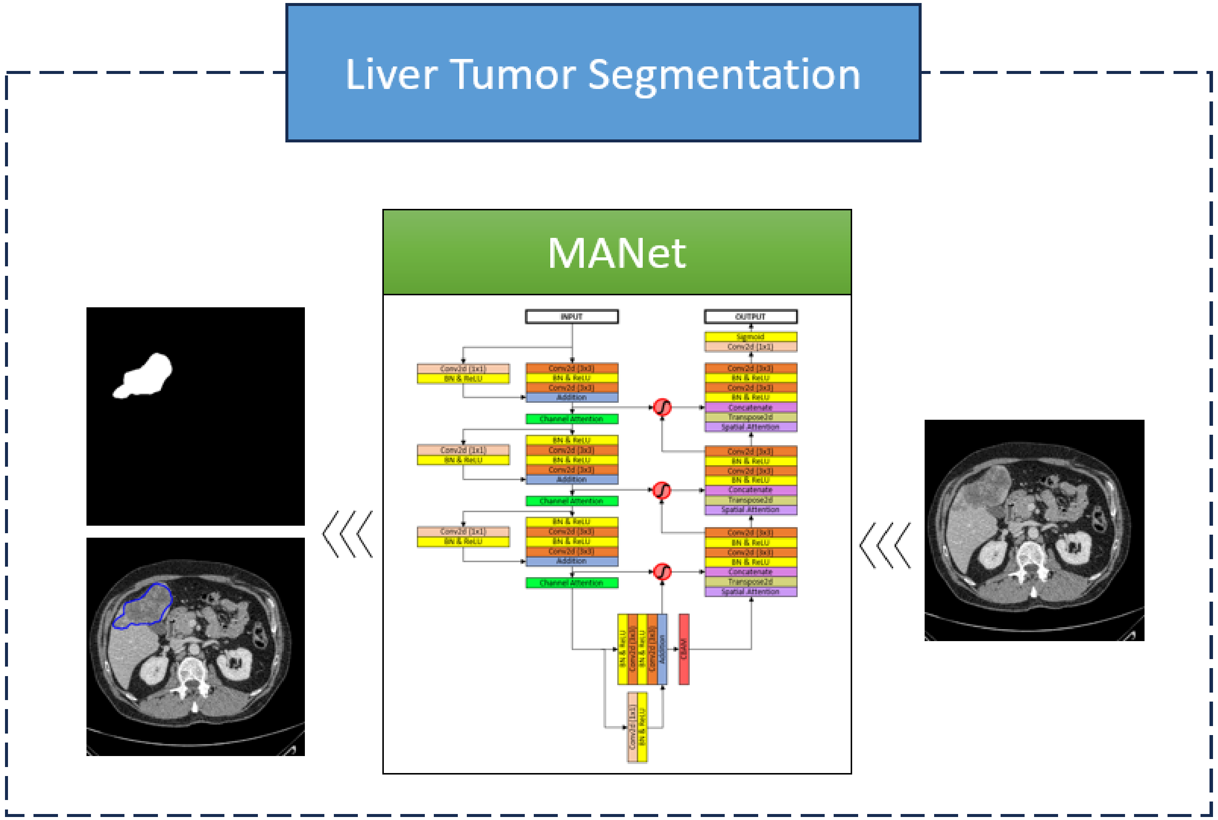

Proposed Method: Novel Architecture Design

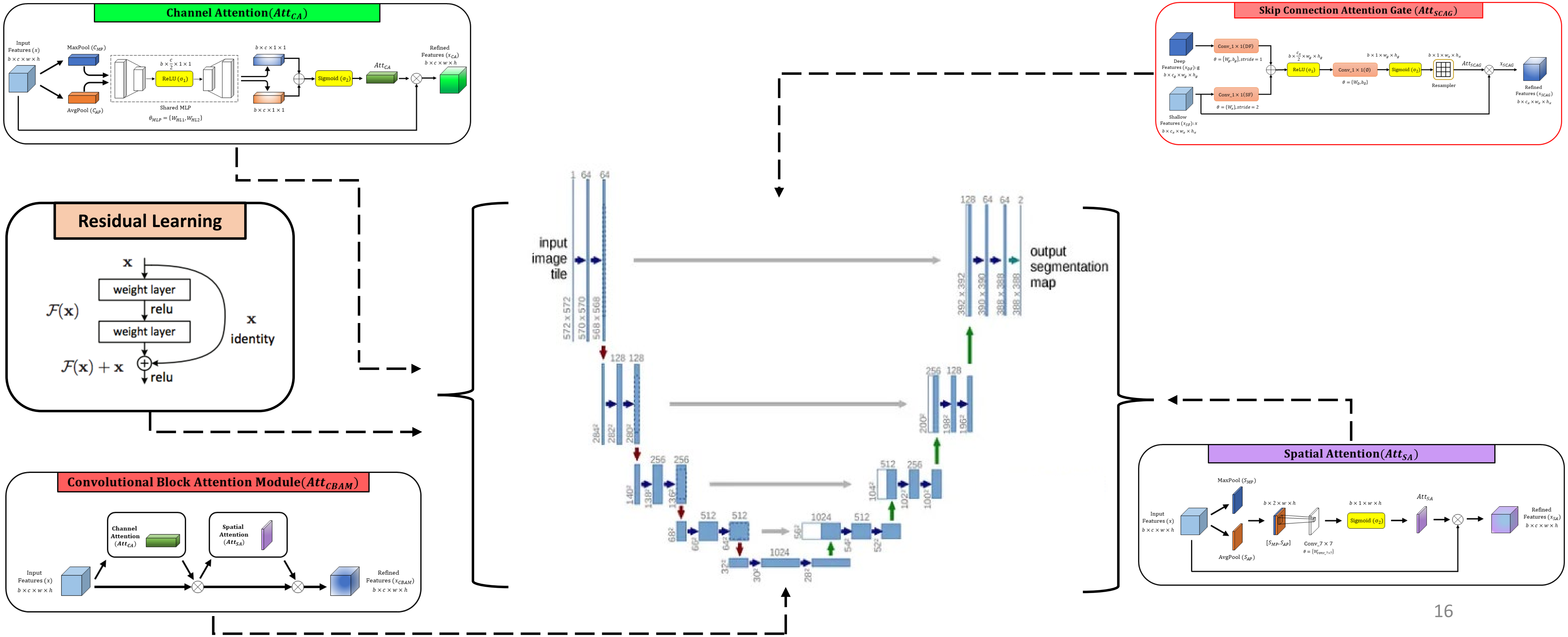

Proposed Method: Novel Architecture Design

MANet: a multi-attention network

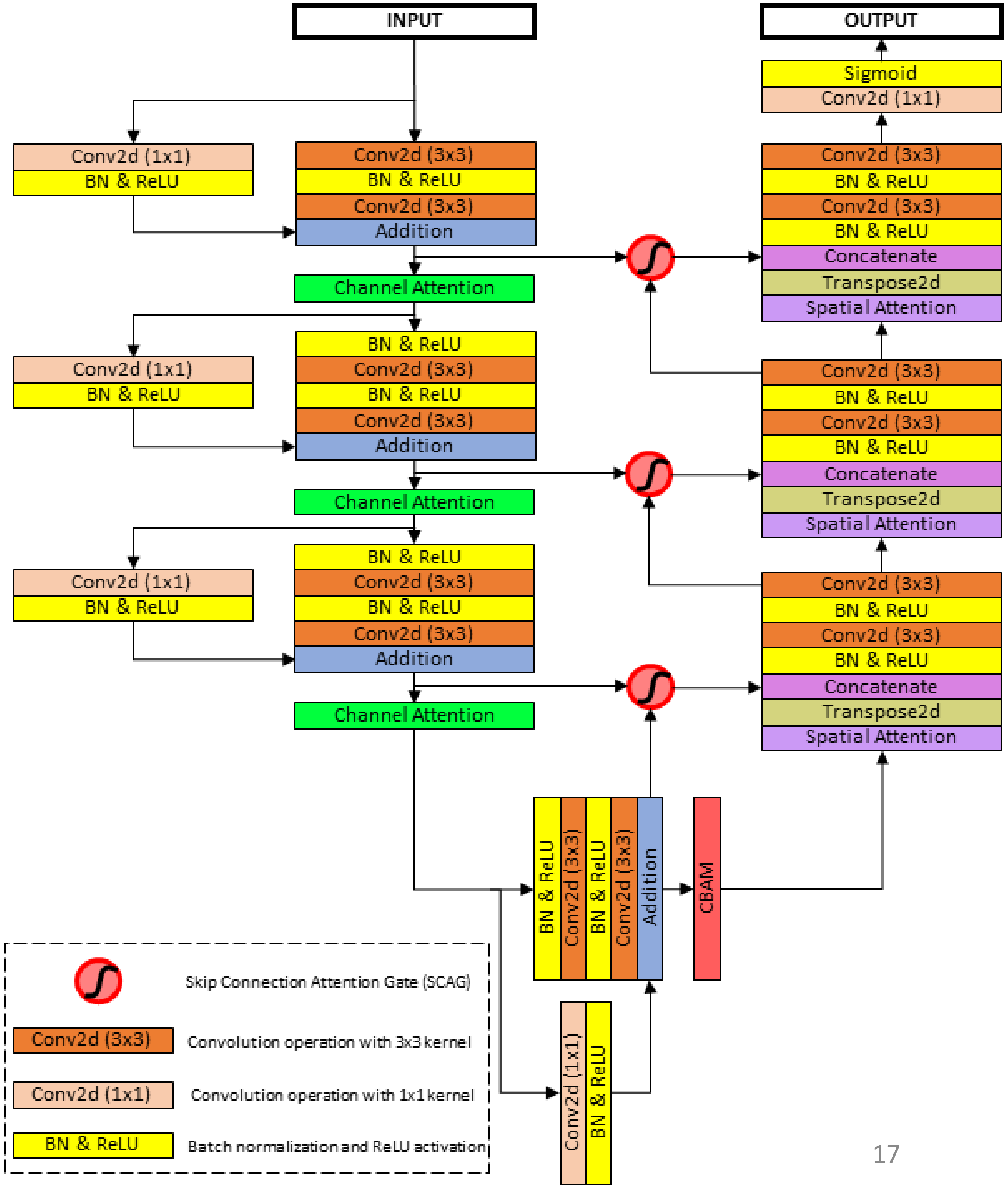

Proposed Method: Novel Architecture Design

MANet: a multi-attention network

Block name	Operation	Filter size	Number of filters	Stride	Output size
Input Image					512 × 512 × 3
Encoder 1	Conv 1	3 × 3	68	1	512 × 512 × 68
	Conv 2	3 × 3	68	1	512 × 512 × 68
Encoder 2	Conv 3	3 × 3	136	2	256 × 256 × 136
	Conv 4	3 × 3	136	1	256 × 256 × 136
Encoder 3	Conv 5	3 × 3	272	2	128 × 128 × 272
	Conv 6	3 × 3	272	1	128 × 128 × 272
Bridge	Conv 7	3 × 3	544	2	64 × 64 × 544
	Conv 8	3 × 3	544	1	64 × 64 × 544
Decoder 1	Conv 9	3 × 3	136	1	128 × 128 × 136
	Conv 10	3 × 3	136	1	128 × 128 × 136
Decoder 2	Conv 11	3 × 3	68	1	256 × 256 × 68
	Conv 12	3 × 3	68	1	256 × 256 × 68
Decoder 3	Conv 13	3 × 3	68	1	512 × 512 × 68
	Conv 14	3 × 3	34	1	512 × 512 × 34
Output	Conv 15	1 × 1	3	1	512 × 512 × 3

Proposed Method: Attention mechanisms

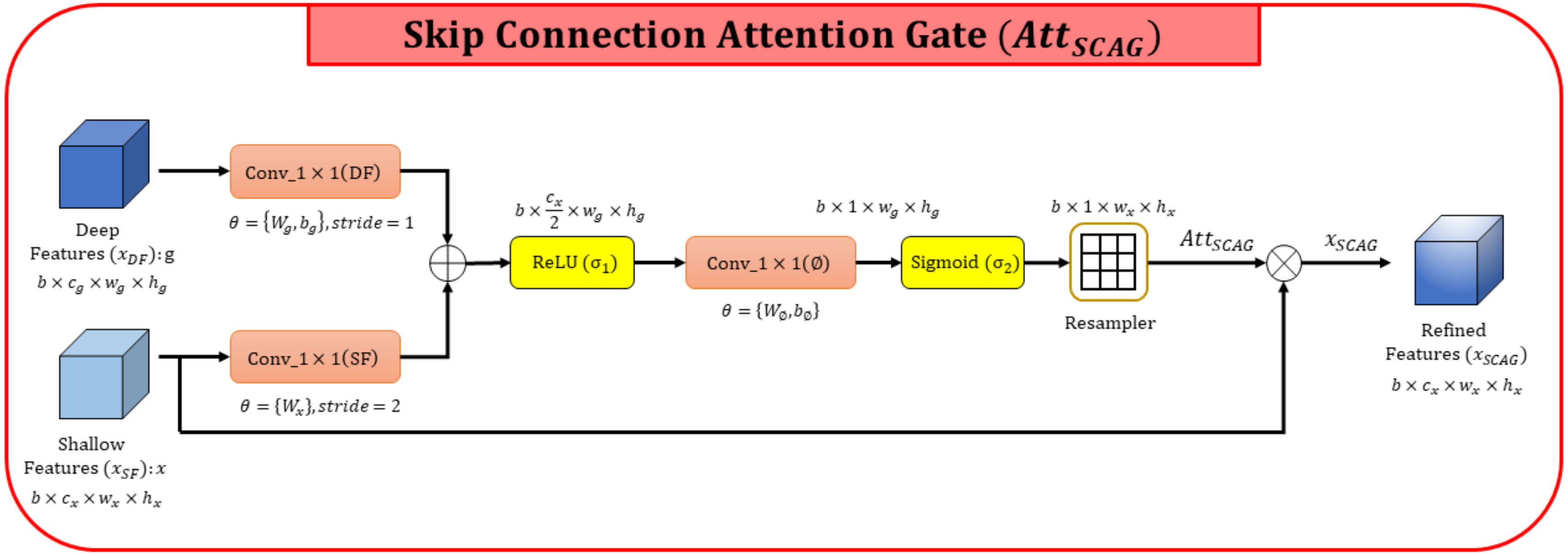

$$x_{conv\_1\times1(SF)} = W_x . x_{SF}$$
$$x_{SF} \in \mathbb{R}^{b\times c_x\times w_x\times h_x}$$
$$x_{conv\_1\times1(SF)} \in \mathbb{R}^{b\times c_x/2\times w_g\times h_g}$$

$$x_{conv\_1\times1(DF)} = W_g . x_{DF} + b_g$$
$$x_{DF} \in \mathbb{R}^{b\times c_g\times w_g\times h_g}$$
$$x_{conv\_1\times1(DF)} \in \mathbb{R}^{b\times c_x/2\times w_g\times h_g}$$

- **Skip Connection Attention Gate (*Att_{SCAG}*)**

$$Att_{SCAG}(x_{SF}, x_{DF}, \theta_{SCAG}) = \sigma_2\left(W_Ø . \sigma_1\left(x_{conv\_1\times1(SF)} + x_{conv\_1\times1(DF)}\right) + b_Ø\right)$$

$$x_{SCAG} = x_{SF} \otimes Att_{SCAG}(x_{SF}, x_{DF}; \theta_{SCAG})$$

$$x_{SCAG} \in \mathbb{R}^{b\times c_x\times w_x\times h_x}$$

Proposed Method: Attention mechanisms

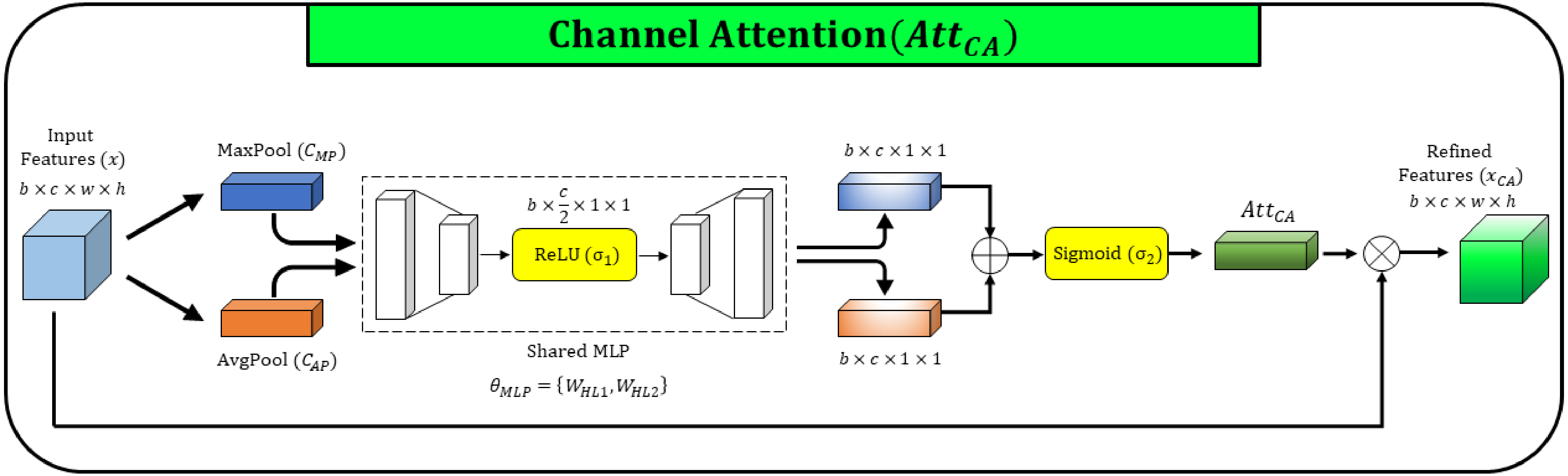

- **Channel Attention (Att_{CA})**

$$Att_{CA}(x;\ \theta_{CA}) = \sigma_2\big(MLP(C_{MP}) + MLP(C_{AP})\big)$$

$$x_{CA} = x \otimes Att_{CA}(x;\ \theta_{CA}),\ x_{CA} \in \mathbb{R}^{b\times c\times w\times h}$$

Where MLP is formulated as follows,

$$MLP(x;\ \theta_{MLP}) = W_{HL2}.\sigma_1(W_{HL1}.x)$$

$$\theta_{CA} = \theta_{MLP} = \{W_{HL1},\ W_{HL2}\}$$

Feature descriptors ($C_{MP}, C_{AP} \in \mathbb{R}^{b\times c\times 1\times 1}$)

$$C_{MP} = MaxPool(x)$$

$$C_{AP} = AvgPool(x)$$

Proposed Method: Attention mechanisms

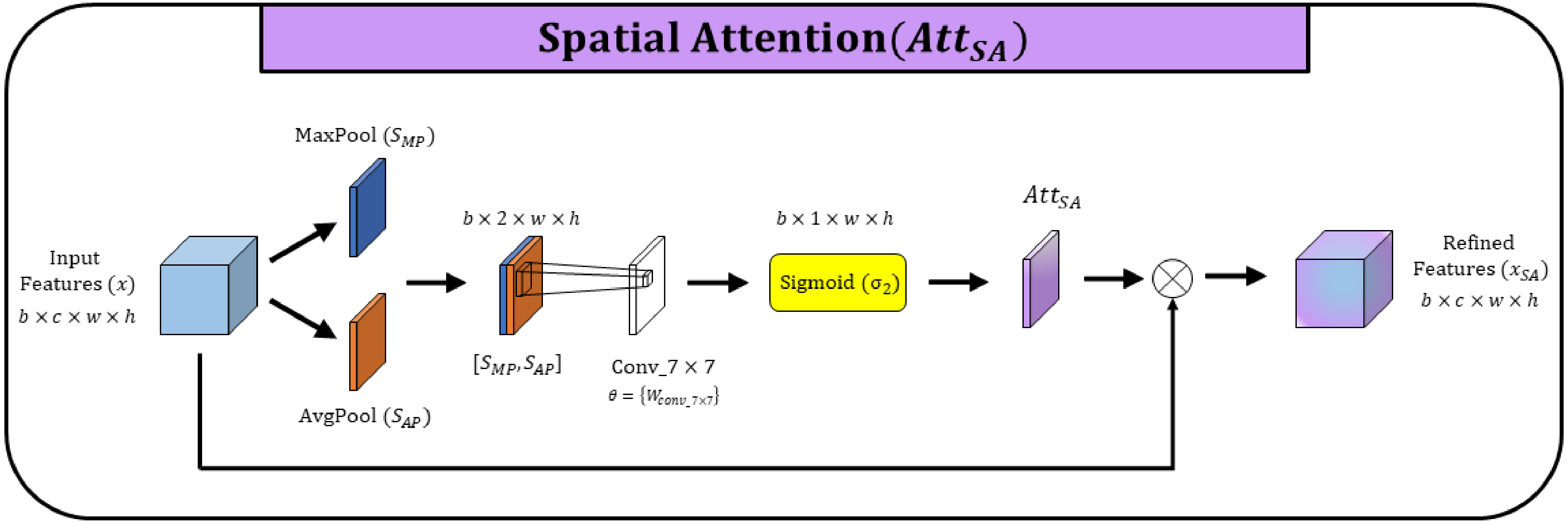

❖ **Spatial Attention (Att_{SA})**

$$Att_{SA}(x;\ \theta_{SA}) = \sigma_2(W_{conv\_7\times7}.([S_{MP},\ S_{AP}]))$$

$$x_{SA} = x \otimes Att_{SA}(x;\ \theta_{SA}),\ x_{SA} \in \mathbb{R}^{b\times c\times w\times h}$$

Proposed Method: Attention mechanisms

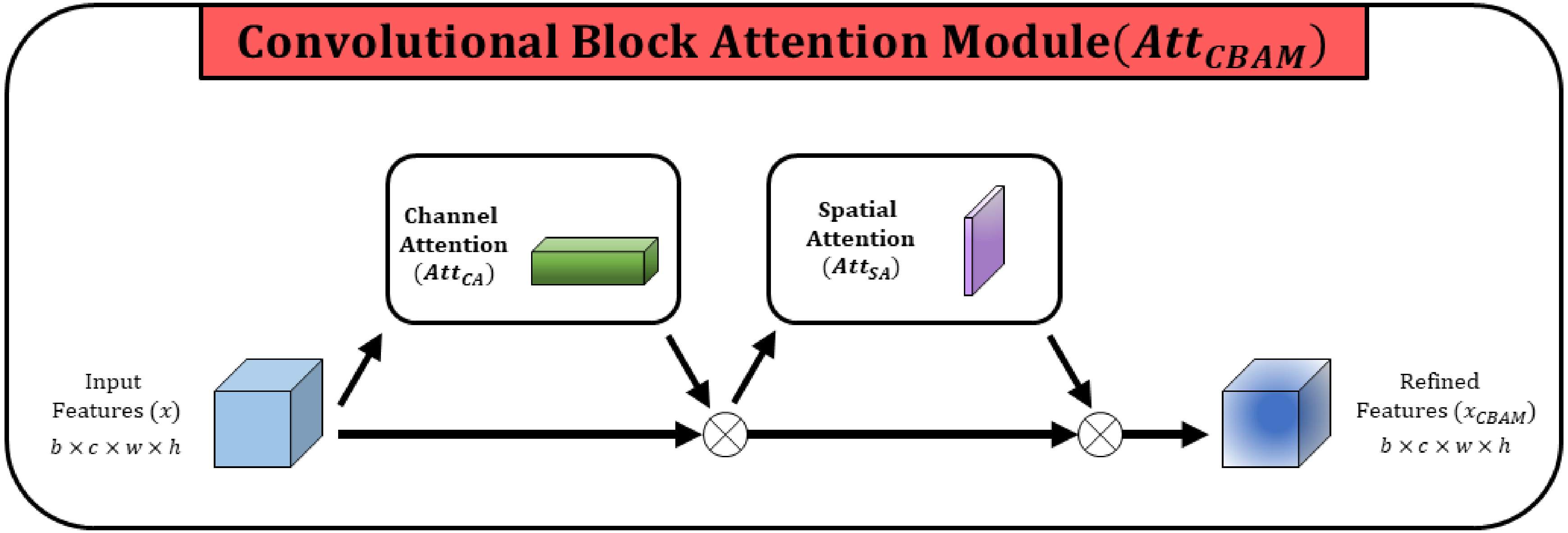

❖ **Convolutional Block Attention Module (Att_{CBAM})**

$$x_{CBAM} = x \otimes Att_{CA}(x;\ \theta_{CA}) \otimes Att_{SA}(x \otimes Att_{CA}(x;\ \theta_{CA});\ \theta_{SA})$$

$$x_{CBAM} \in \mathbb{R}^{b \times c \times w \times h}$$

Proposed Method: Concept formation

- UNet performed well in medical image segmentation[1].
- UNet is designed with skip connection[1].
- Each block is limited to two convolution layers[2].
- Batch normalization can improve the learning process[3].
- The combination of BN & ReLU can address the gradient vanishment issue[3].
- Residual learning can minimize the learning errors to address degradation issue[2].

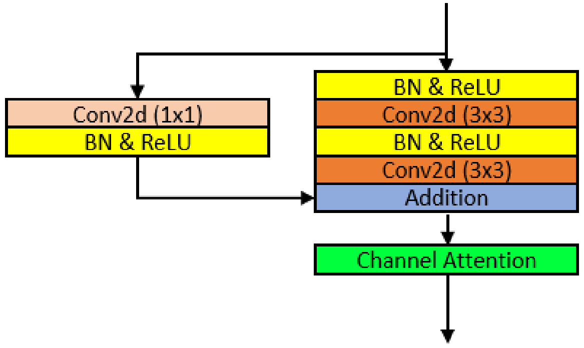

Encoder Block

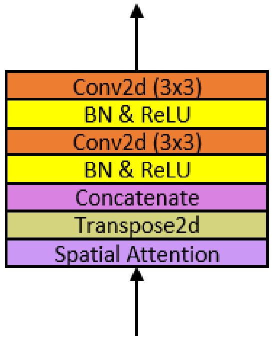

Decoder Block

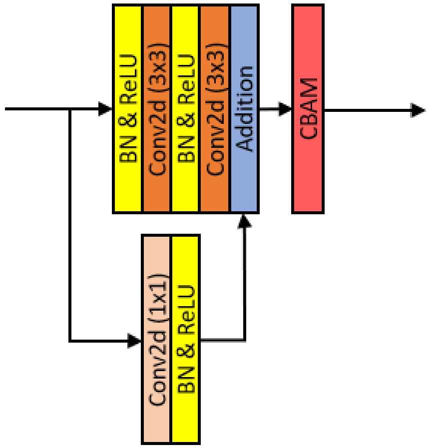

Bridge Block

[1]Ronneberger, O., Fischer, P. & Brox, T. U-net: Convolutional networks for biomedical image segmentation. In Medical Image Computing and Computer-Assisted Intervention - MICCAI 2015 (eds Navab, N., Hornegger, J., Wells, W. M. & Frangi, A. F.) 234–241 (Springer International Publishing, Cham, 2015).

[2]He, K., Zhang, X., Ren, S. & Sun, J. Deep residual learning for image recognition. In 2016 IEEE Conference on Computer Vision and Pattern Recognition (CVPR) 770–778 https:// doi. org/ 10. 1109/ CVPR. 2016. 90 (2016).

[3]https://medium.com/analytics-vidhya/how-batch-normalization-and-relu-solve-vanishing-gradients-3f1a8ace1c88

Experimental setup: Dataset

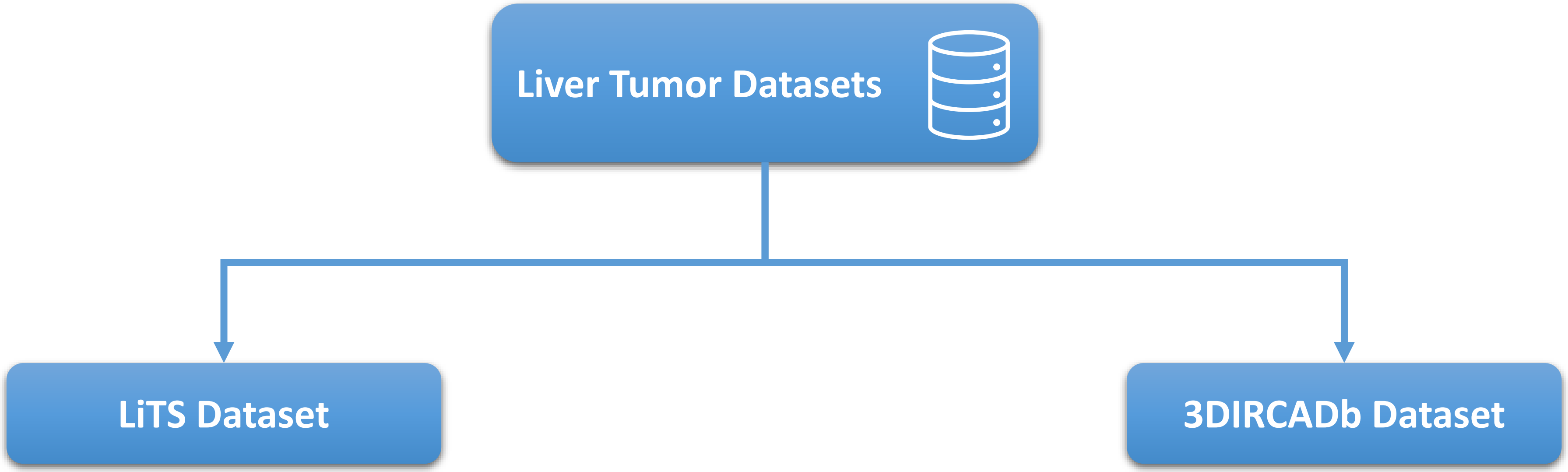

[1]Bilic, P. et al. The liver tumor segmentation benchmark (LiTS). Med. Image Analysis 84, 102680, DOI: 10.1016/j.media.2022.102680 (2023).

[2]Soler, L. et al. 3D Image Reconstruction for Comparison of Algorithm Database: A Patient Specific Anatomical and Medical Image

Experimental setup: Dataset

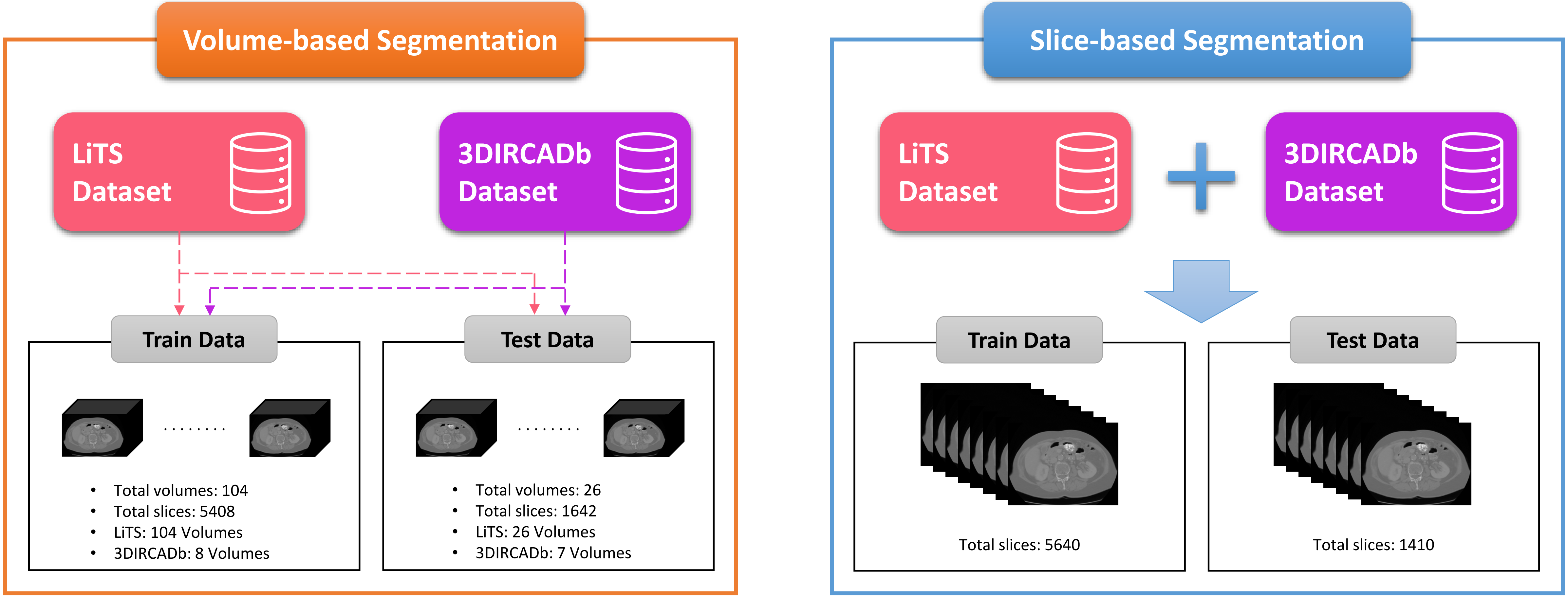

Experimental setup: System overview

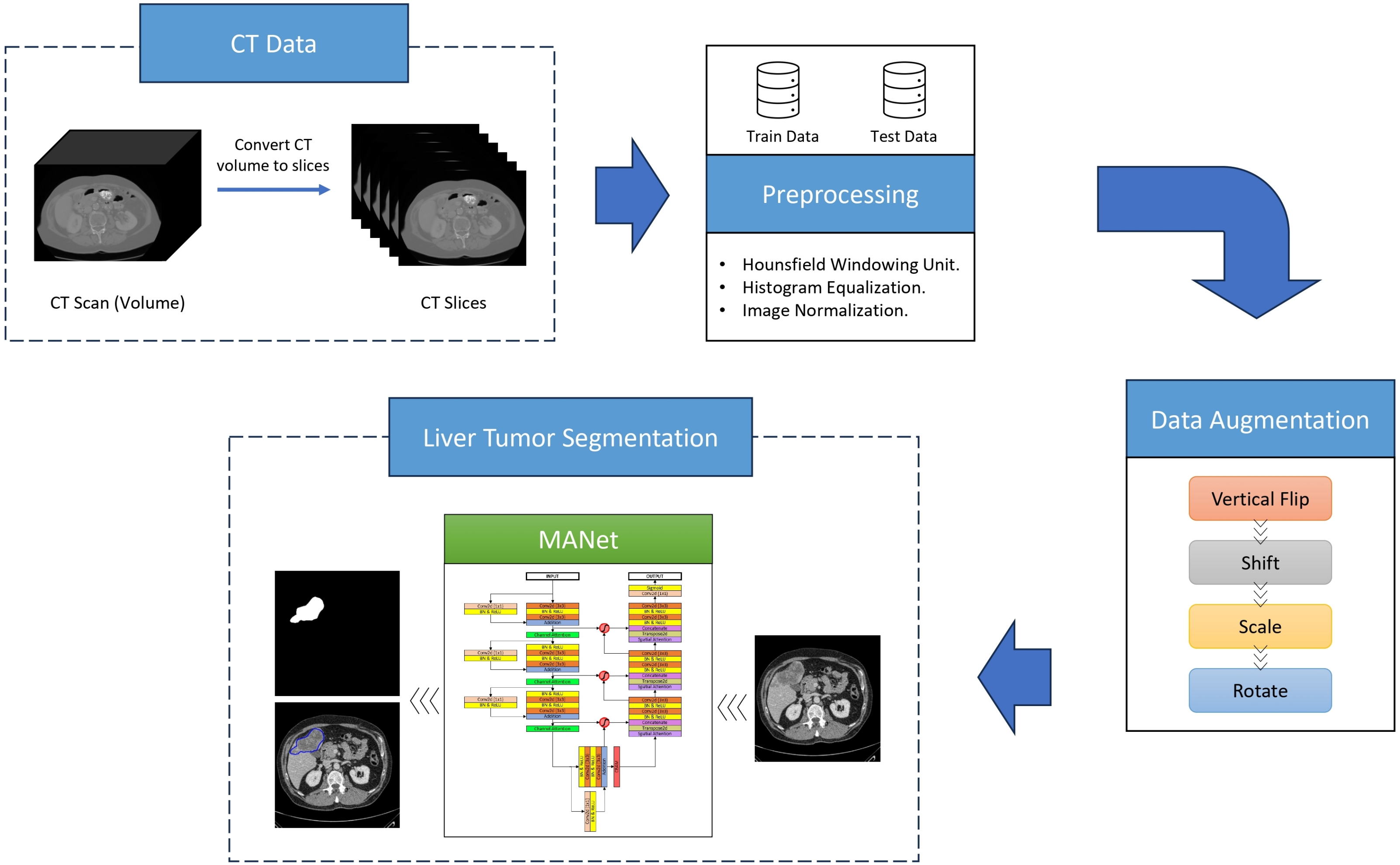

Experimental setup: Model training setup

Loss Function

- Dice loss is designed to calculate the overlap between two samples.
- The measuring range of the Dice score is 0 to 1.
- Perfect overlap gives Dice score 1. Dice loss function gives 0 (Zero error)
- When the overlapping is maximized, the dice loss is minimized.

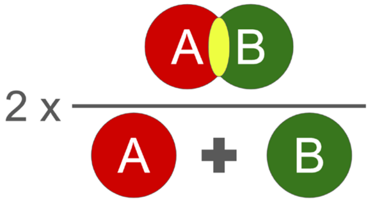

$$DICE = \frac{2|A \cap B|}{|A| + |B|} \qquad DICE\ Loss = 1 - DICE$$

Training setup

- Optimizer: Adam
- Learning rate: 1e-4
- Learning rate is attenuated by 0.1 in every 30 epochs
- Total epochs: 80
- Batch size: 8

Implementation details

- CPU: Intel(R) Core (TM) i7-9750H (6 cores)
- GPU: RTX2070 (8 GB)
- RAM: 32 GB

Experimental setup: Evaluation metrics

$$DICE = \frac{2|A \cap B|}{|A| + |B|} = \frac{2TP}{2TP + FP + FN}$$

$$Jaccard\ index = IoU = \frac{|A \cap B|}{|A \cup B|} = \frac{TP}{TP + FP + FN}$$

$$VOE = 1 - \frac{|A \cap B|}{|A \cup B|} = 1 - Jaccard\ index$$

$$Accuracy = \frac{TP + TN}{TP + TN + FP + FN}$$

$$Sensitivity\ (Recall) = \frac{TP}{TP + FN}$$

$$Specificity = \frac{TN}{TN + FP}$$

$$ASSD = \frac{\sum_{x \in \partial B} d(x, \partial A) + \sum_{y \in \partial A} d(y, \partial B)}{|\partial B| + |\partial A|}$$

04 Experimental Results

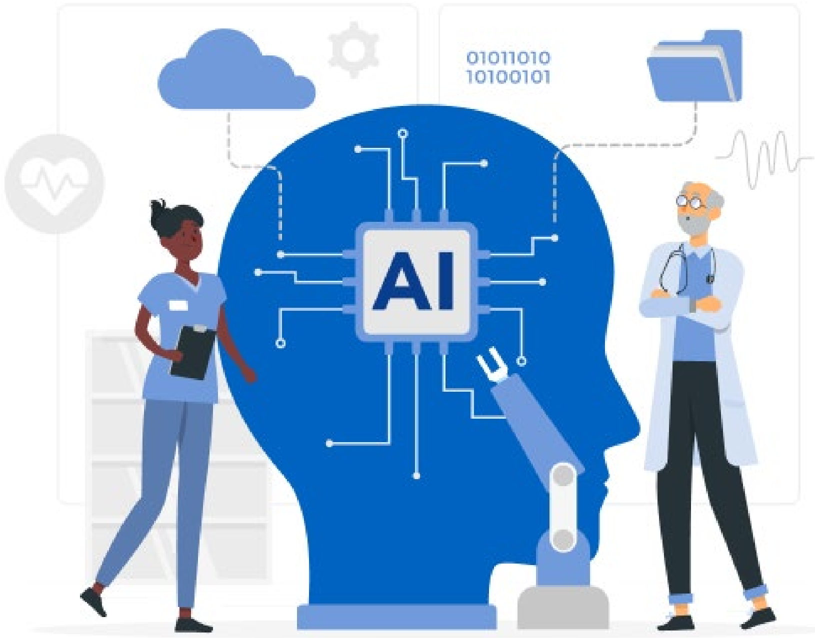

Experimental Results

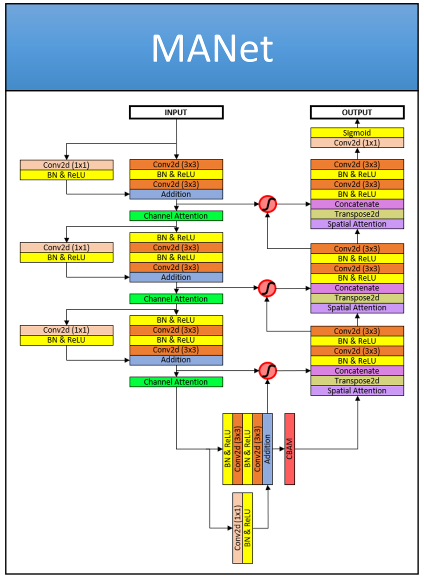

- Quantitative Analysis of Segmentation Performance
- Quantitative Analysis based on the Number of Tumors
- Quantitative Analysis based on the Total Area of Tumors
- Liver Tumor Segmentation Validation with a Radiologist
- Qualitative Analysis of Segmentation Mask
- Model Feature Visualization
- Computational Cost Analysis
- Ablation Analysis

Quantitative Analysis of Segmentation Performance

Quantitative Analysis of Segmentation Performance
(LiTS Dataset)

Volume-based and slice-based segmentation experiments on the LiTS dataset.

Task	Methods	Dice score	ASSD	Jaccard index (IoU)	VOE	Accuracy	Sensitivity (Recall)	Specificity
Volume-based Segmentation	UNet	0.6612 ± 0.277	1.0843 ± 1.425	0.5469 ± 0.266	0.4530 ± 0.266	**0.9950 ± 0.004**	0.6394 ± 0.285	0.9987 ± 0.002
	Attention UNet	0.6505 ± 0.278	1.2551 ± 1.338	0.5356 ± 0.263	0.4643 ± 0.263	0.9945 ± 0.006	0.6250 ± 0.292	0.9984 ± 0.002
	UNet + Resnet18	0.6560 ± 0.281	**0.9321 ± 0.960**	0.5433 ± 0.268	0.4566 ± 0.268	0.9950 ± 0.005	0.6108 ± 0.294	**0.9991 ± 0.001**
	UNet + CBAM	0.6635 ± 0.271	1.2795 ± 1.638	0.5487 ± 0.261	0.4512 ± 0.261	0.9946 ± 0.005	0.6678 ± 0.283	0.9981 ± 0.002
	MANet (Proposed model)	**0.6735 ± 0.267**	1.2049 ± 1.356	**0.5590 ± 0.258**	**0.4409 ± 0.258**	**0.9950 ± 0.004**	**0.7426 ± 0.283**	0.9978 ± 0.002
Slice-based segmentation	UNet	0.7790 ± 0.208	0.9009 ± 1.020	0.6744 ± 0.217	0.3255 ± 0.217	0.9940 ± 0.006	0.7476 ± 0.237	0.9982 ± 0.001
	Attention UNet	0.7676 ± 0.195	0.9188 ± 0.783	0.6550 ± 0.208	0.3449 ± 0.208	0.9935 ± 0.006	0.7423 ± 0.231	0.9978 ± 0.002
	UNet + Resnet18	0.7686 ± 0.211	1.0037 ± 1.4291	0.6619 ± 0.223	0.3380 ± 0.223	0.9934 ± 0.007	0.7342 ± 0.245	**0.9984 ± 0.001**
	UNet + CBAM	0.7784 ± 0.202	0.8241 ± 0.810	0.6720 ± 0.214	0.3279 ± 0.214	0.9941 ± 0.005	0.7439 ± 0.234	0.9982 ± 0.002
	MANet (Proposed model)	**0.8145 ± 0.150**	**0.7084 ± 0.701**	**0.7084 ± 0.171**	**0.2915 ± 0.171**	**0.9947 ± 0.004**	**0.8723 ± 0.173**	0.9970 ± 0.002

Table 5.1: Volume-based and slice-based segmentation experiments (mean ± standard deviation) on the LiTS dataset. The best values are in bold.

Quantitative Analysis of Segmentation Performance (LiTS Dataset)

Volume-based segmentation experiments on the LiTS dataset.

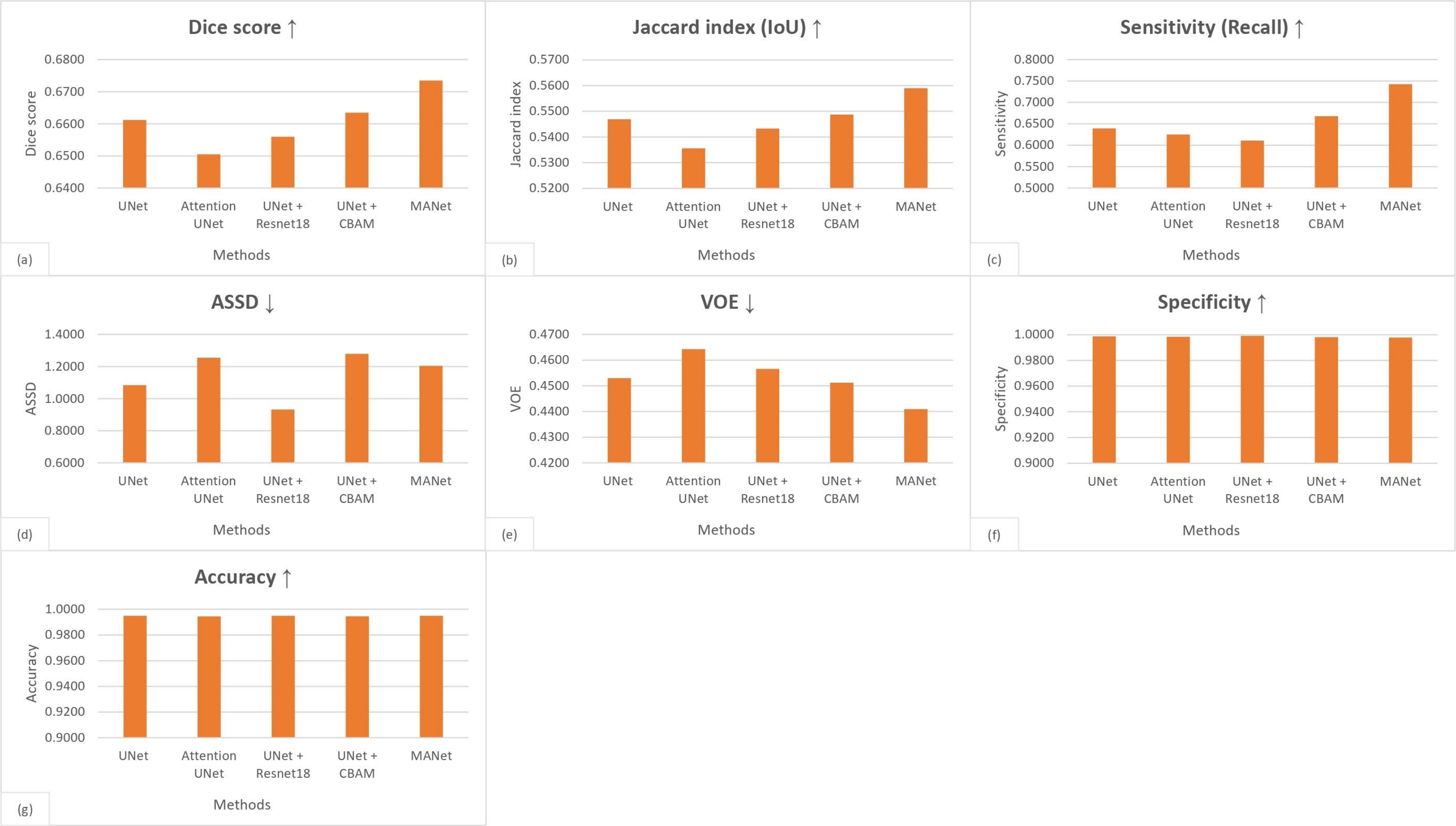

(a) Dice score,

(b) Jaccard index (IoU),

(c) Sensitivity (Recall),

(d) ASSD,

(e) VOE,

(f) Specificity,

(g) Accuracy.

Quantitative Analysis of Segmentation Performance
(LiTS Dataset)

Slice-based segmentation experiments on the LiTS dataset.

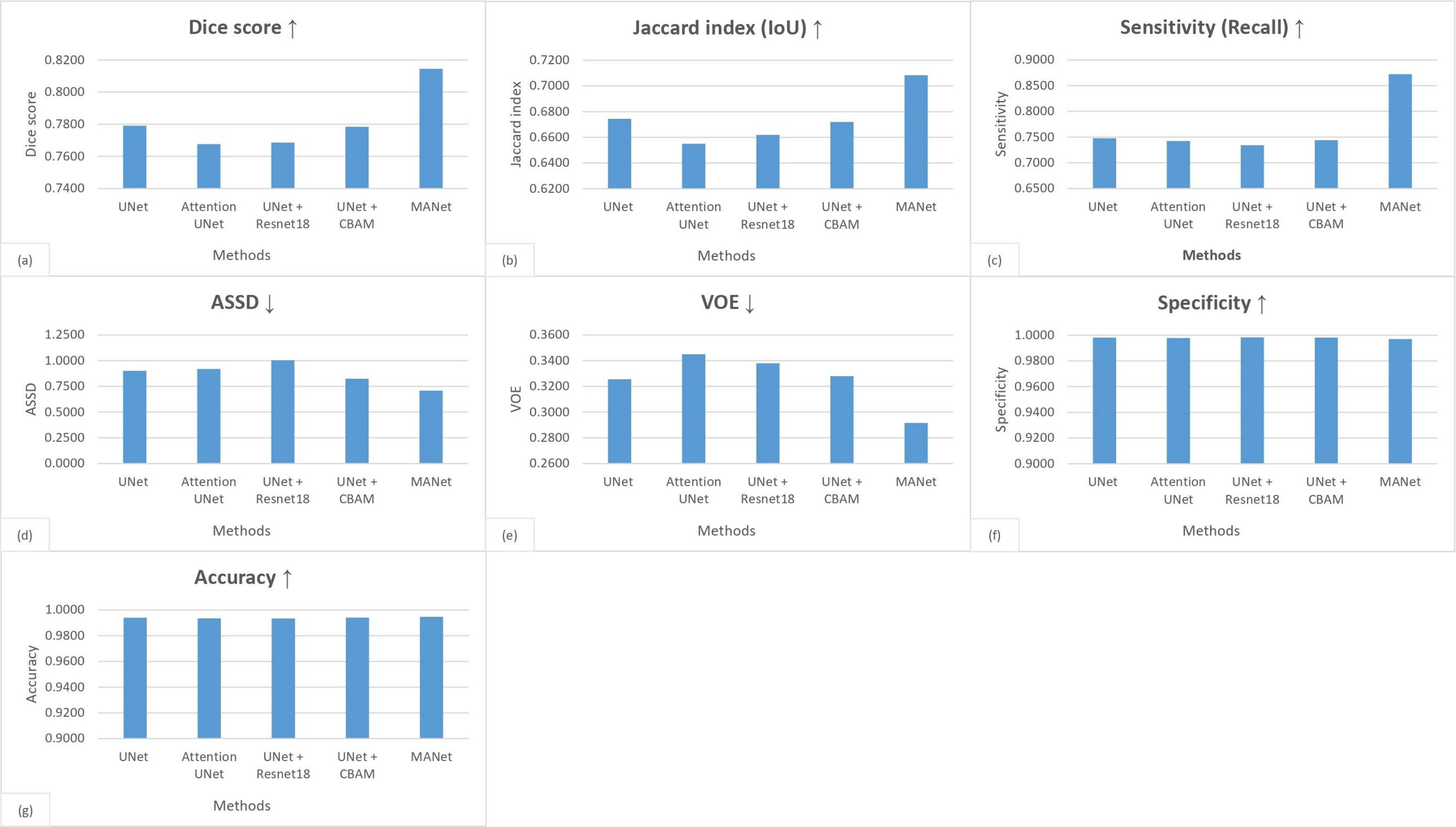

(a) Dice score,

(b) Jaccard index (IoU),

(c) Sensitivity (Recall),

(d) ASSD,

(e) VOE,

(f) Specificity,

(g) Accuracy.

Quantitative Analysis of Segmentation Performance
(LiTS Dataset)

Volume-based and slice-based segmentation experiments on the LiTS dataset.

(a) Dice score,

(b) Jaccard index (IoU),

(c) Sensitivity (Recall),

(d) ASSD,

(e) VOE,

(f) Specificity,

(g) Accuracy.

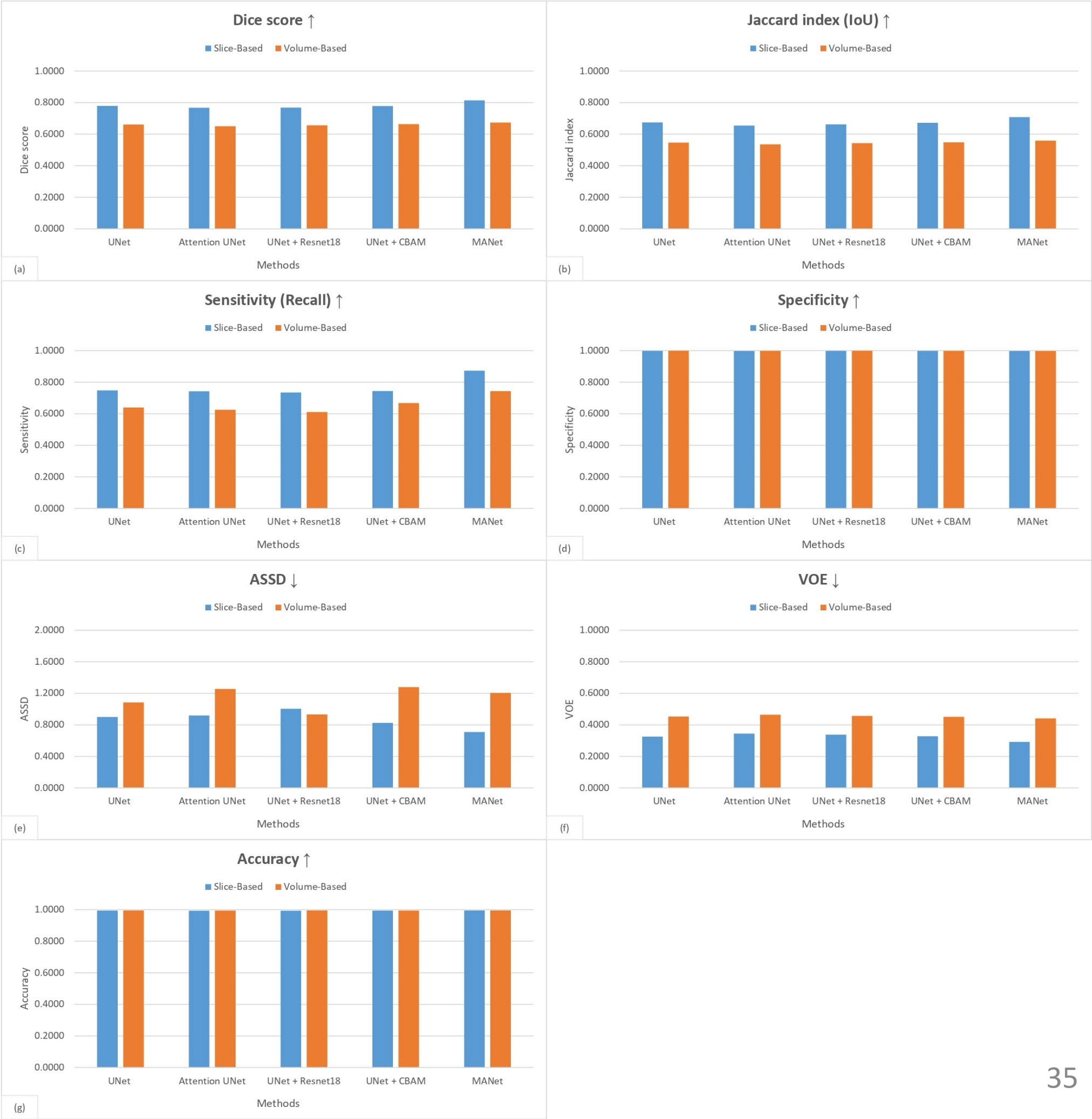

Quantitative Analysis of Segmentation Performance
(LiTS Dataset)

Quantitative Analysis based on the Performance Rating

- Dice score
- Jaccard index (IoU)
- Sensitivity (Recall)

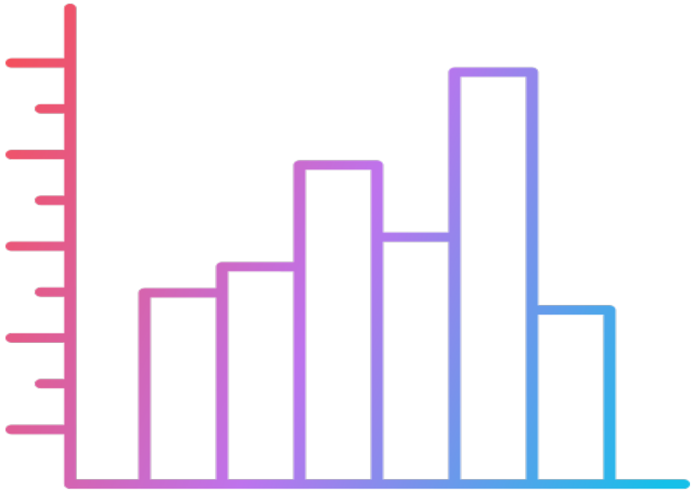

Segmentation Rating	Performance Range (%)
1	0 % - 20 %
2	20 % - 40 %
3	40 % - 60 %
4	60 % - 80 %
5	80 % - 100 %

Table 5.2: The quantitative segmentation rating.

Quantitative Analysis of Segmentation Performance
(LiTS Dataset)

Histogram of the quantitative segmentation rating for volume-based segmentation

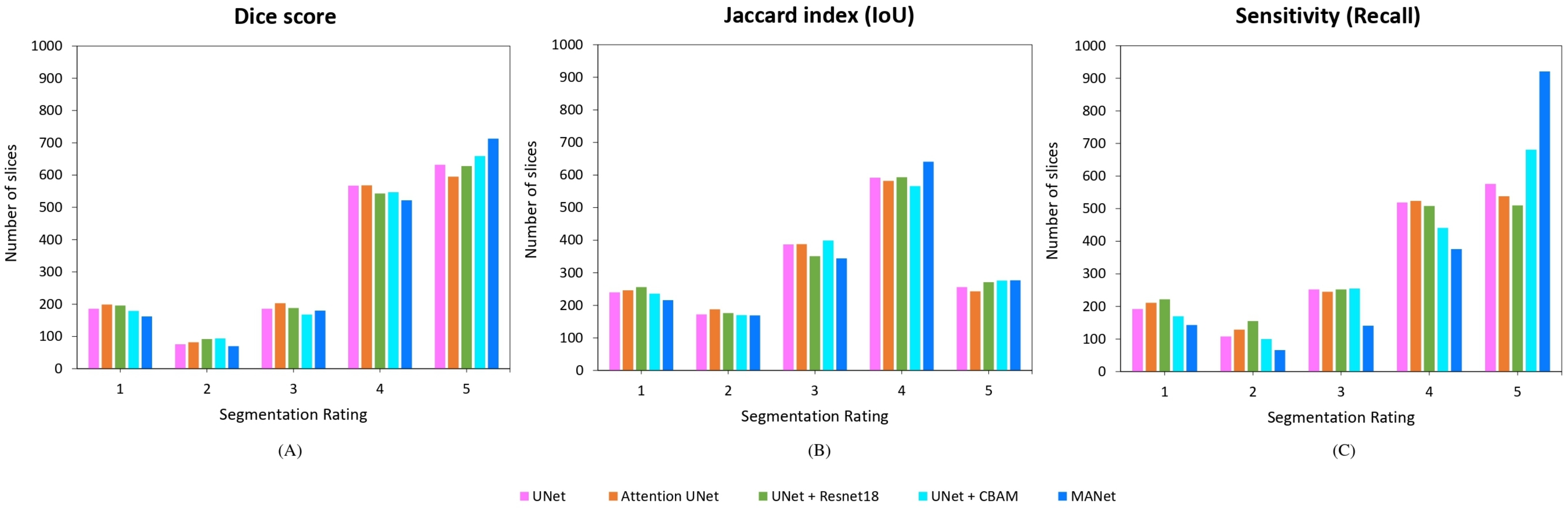

Quantitative Analysis of Segmentation Performance
(LiTS Dataset)

Histogram of the quantitative segmentation rating for slice-based segmentation

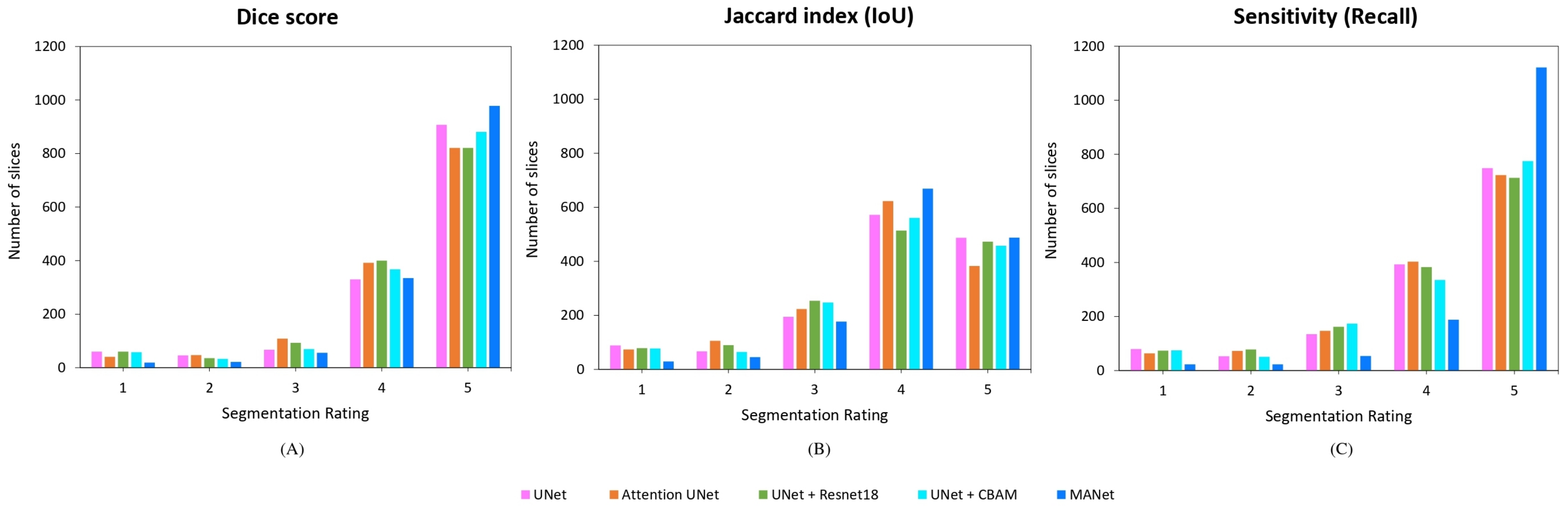

Quantitative Analysis of Segmentation Performance
(3DIRCADb Dataset)

Volume-based segmentation experiments on the 3DIRCADb dataset.

Methods	Dice score	ASSD	Jaccard index (IoU)	VOE	Accuracy	Sensitivity (Recall)	Specificity
UNet	0.5767 ± 0.282	1.2578 ± 1.199	0.4534 ± 0.246	0.5466 ± 0.246	0.9942 ± 0.006	0.4813 ± 0.253	0.9996 ± 0.001
Attention UNet	0.5863 ± 0.281	1.4189 ± 1.288	0.4629 ± 0.245	0.5371 ± 0.245	0.9943 ± 0.006	0.4954 ± 0.259	0.9995 ± 0.001
UNet + Resnet18	0.5941 ± 0.270	**1.2051 ± 1.038**	0.4681 ± 0.241	0.5319 ± 0.241	0.9944 ± 0.006	0.4956 ± 0.256	**0.9997 ± 0.001**
UNet + CBAM	0.5763 ± 0.278	1.5157 ± 1.458	0.4521 ± 0.246	0.5479 ± 0.246	0.9941 ± 0.006	0.4909 ± 0.257	0.9995 ± 0.001
MANet (Proposed model)	**0.6400 ± 0.279**	1.3492 ± 1.362	**0.5227 ± 0.258**	**0.4773 ± 0.258**	**0.9947 ± 0.006**	**0.6240 ± 0.298**	0.9990 ± 0.002

Table 5.3: Volume-based segmentation experiments (mean ± standard deviation) on the 3DIRCADb dataset. The best values are in bold.

Quantitative Analysis of Segmentation Performance

Volume-based segmentation on the LiTS and 3DIRCADb datasets

(a) Dice score,

(b) Jaccard index (IoU),

(c) Sensitivity (Recall),

(d) ASSD,

(e) VOE,

(f) Specificity,

(g) Accuracy.

Quantitative Analysis of Segmentation Performance
(LiTS Dataset)

Performance comparison of MANet model and other state-of-the-art methods for slice-based segmentation experiments on the LiTS dataset.

Methods	Dice score	ASSD	Jaccard index (IoU)	VOE	Accuracy	Sensitivity (Recall)	Specificity	Total training parameters (M)
UNet 3+	0.5036 ± 0.341	1.3994 ± 1.857	0.4054 ± 0.306	0.5946 ± 0.306	0.9893 ± 0.010	0.4696 ± 0.364	0.9977 ± 0.005	26.98
ResUNet++	0.8101 ± 0.175	1.0323 ± 0.950	0.6727 ± 0.191	0.3273 ± 0.191	0.9937 ± 0.006	0.8330 ± 0.205	0.9968 ± 0.003	4.06
SmaAt-Unet	0.7880 ± 0.185	0.8300 ± 0.955	0.6802 ± 0.202	0.3198 ± 0.202	0.9938 ± 0.007	0.7433 ± 0.218	0.9986 ± 0.002	4.03
TA-Net	0.7904 ± 0.172	0.9331 ± 0.974	0.6799 ± 0.190	0.3202 ± 0.190	0.9937 ± 0.007	0.7751 ± 0.209	0.9979 ± 0.003	29.57
MANet (Proposed model)	**0.8145 ± 0.150**	**0.7084 ± 0.701**	**0.7084 ± 0.171**	**0.2915 ± 0.171**	**0.9947 ± 0.004**	**0.8723 ± 0.173**	**0.9970 ± 0.002**	**7.83**

Table 5.4: Slice-based segmentation experiments (mean ± standard deviation) on the 3DIRCADb dataset. The proposed model results are in bold.

Quantitative Analysis of Segmentation Performance
(LiTS Dataset)

Performance comparison of MANet model and other state-of-the-art methods for slice-based segmentation experiments of on the LiTS dataset.

(a) Dice score,

(b) Jaccard index (IoU),

(c) Sensitivity (Recall),

(d) ASSD,

(e) VOE,

(f) Specificity,

(g) Accuracy.

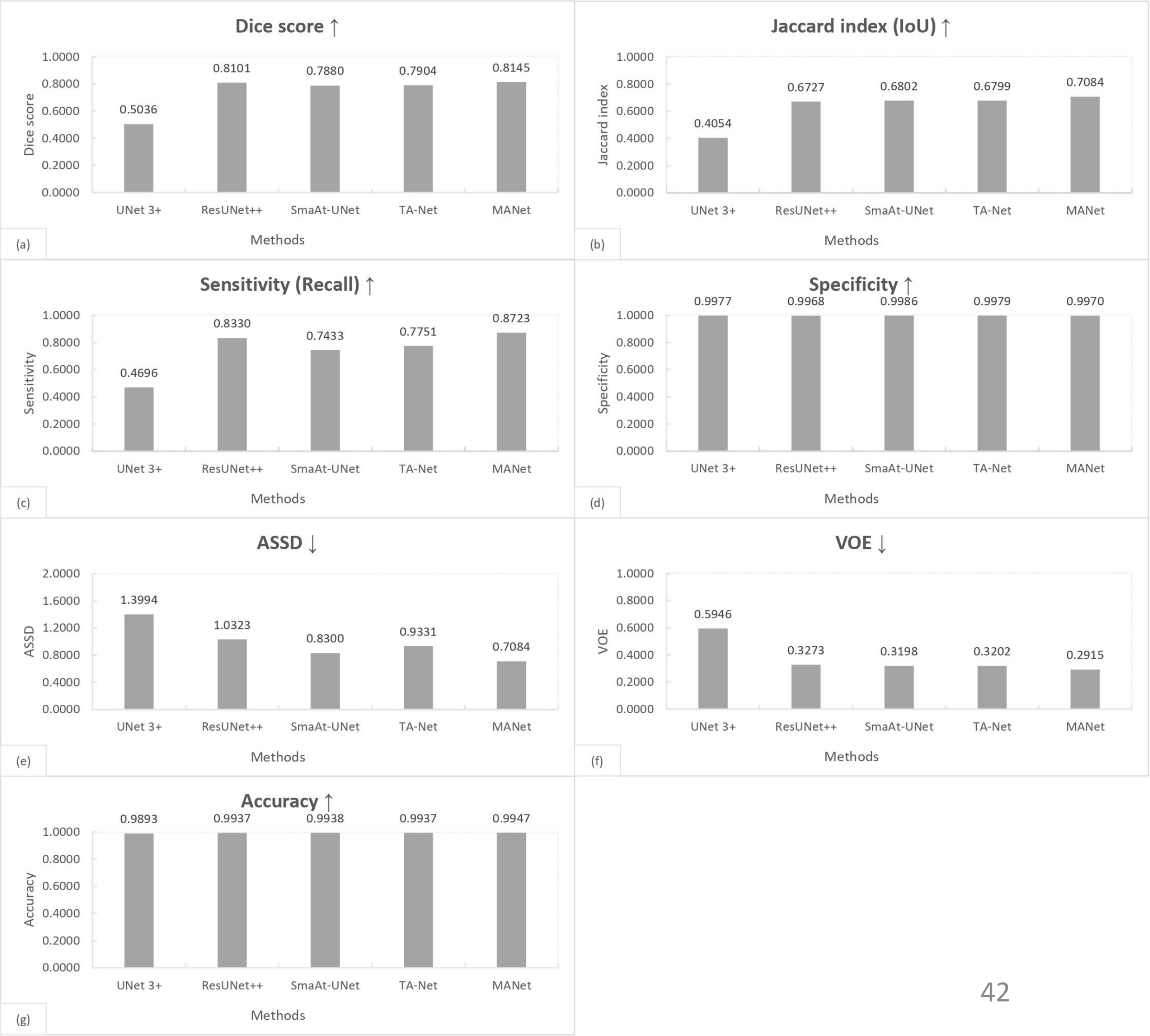

Quantitative Analysis based on the Number of Tumors

Quantitative Analysis based on the Number of Tumors

CT slice data distribution based on the number of liver tumors

Number of Tumors	Number of Slices	Average Total Area of Tumors (mm^2)
1	432	1689
2	285	2842
3	150	3707
4	132	3131
5	96	3983
6	60	3635
7	46	2637
8	33	3495
9	25	3495
10	17	4179
11	14	2808
12	16	3219
13	13	4397
14	12	4537
15	26	5517
> 15	53	6262

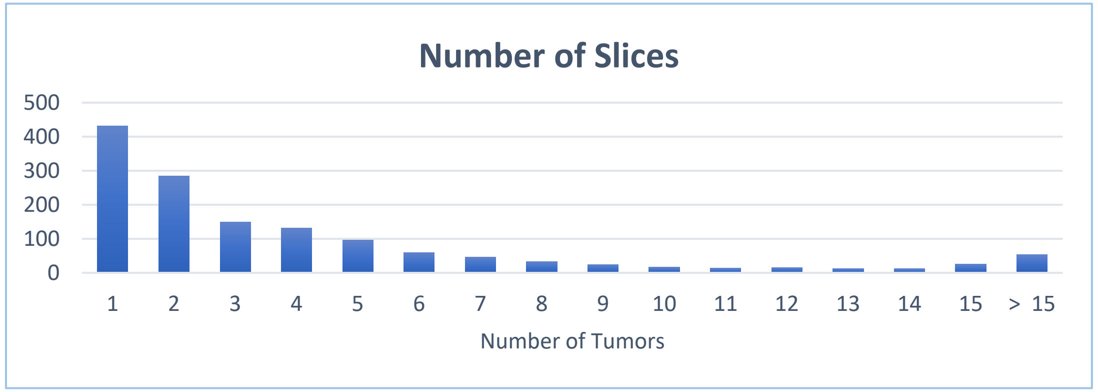

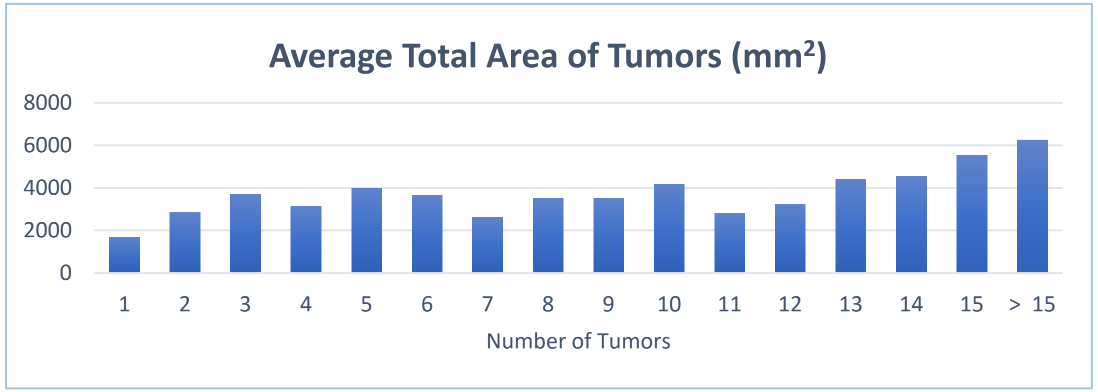

Quantitative Analysis based on the Number of Tumors

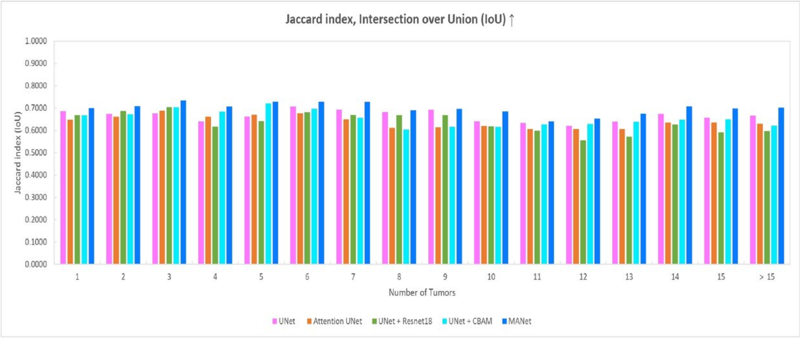

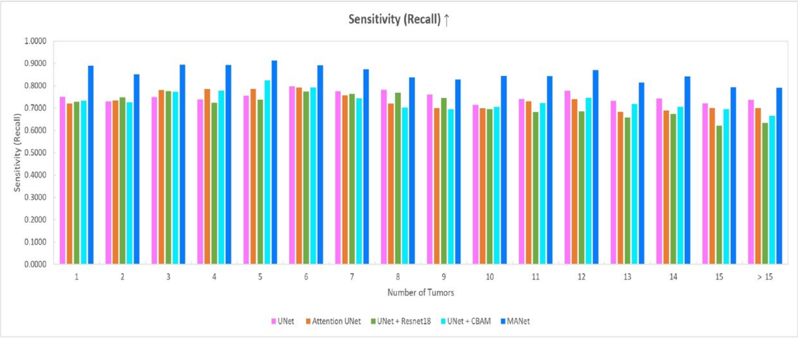

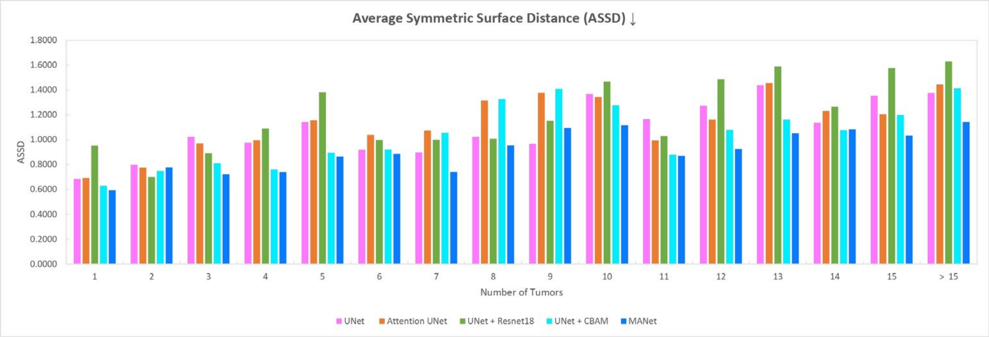

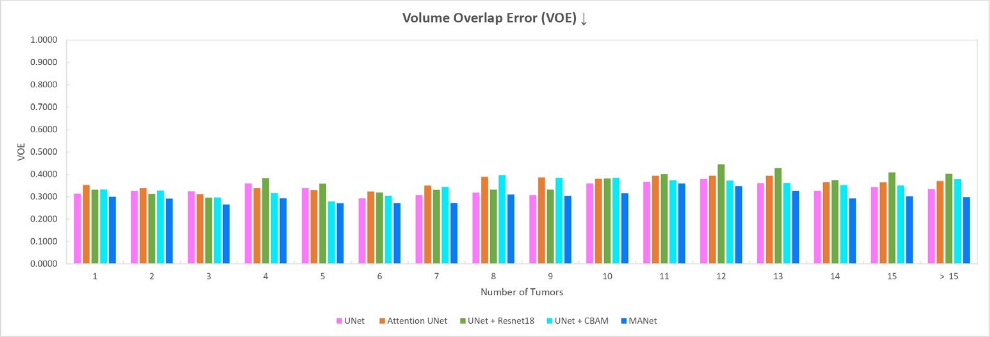

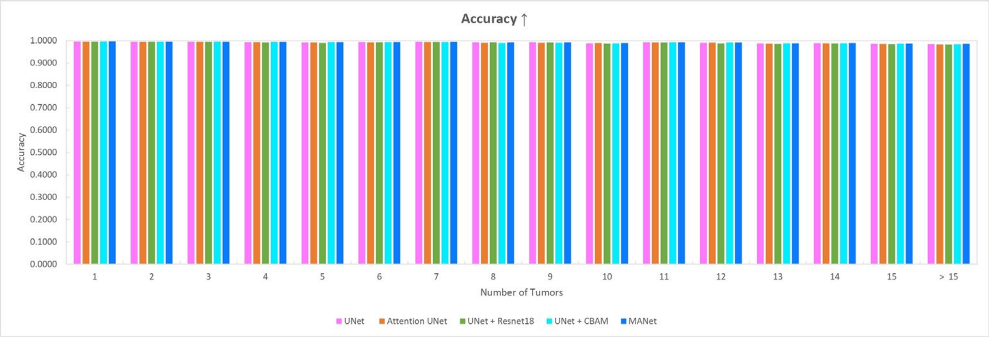

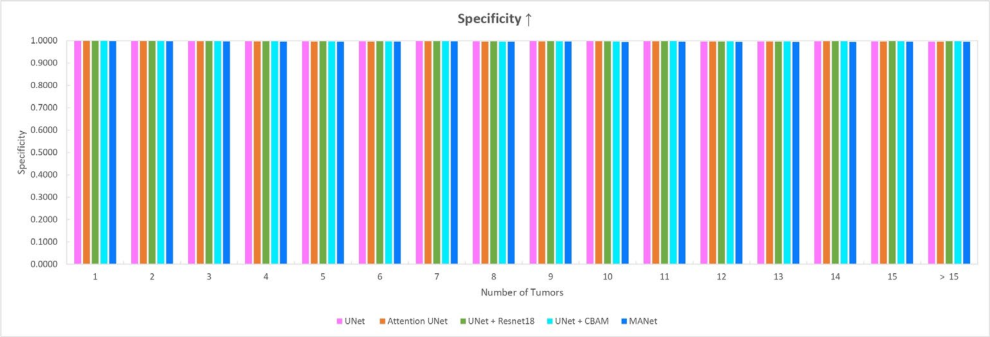

Quantitative Analysis based on the Number of Tumors

Dice score

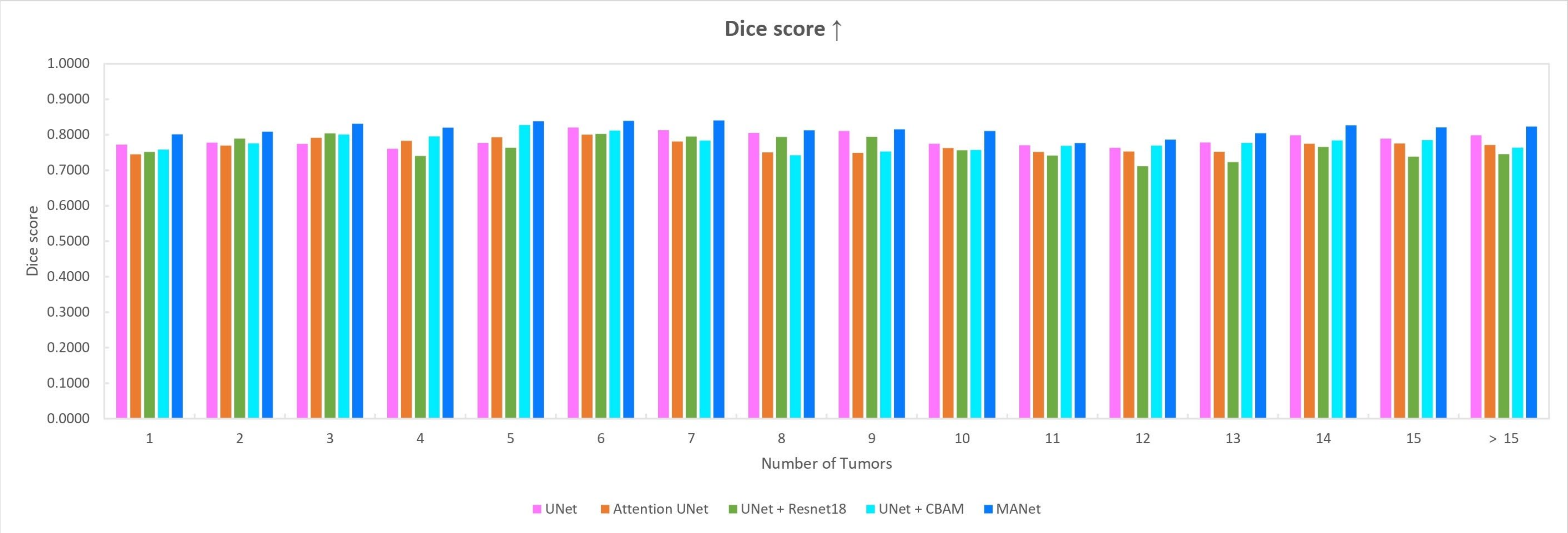

Quantitative Analysis based on the Number of Tumors

Jaccard index, Intersection over Union (IoU)

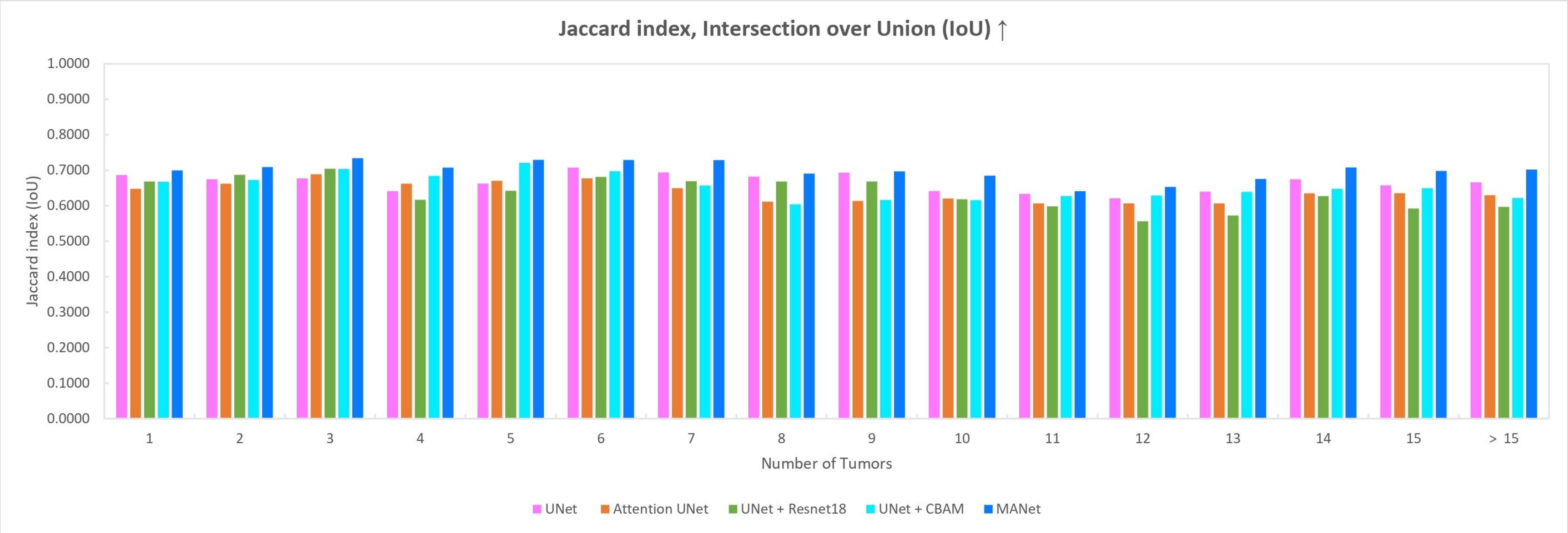

Quantitative Analysis based on the Number of Tumors

Sensitivity (Recall)

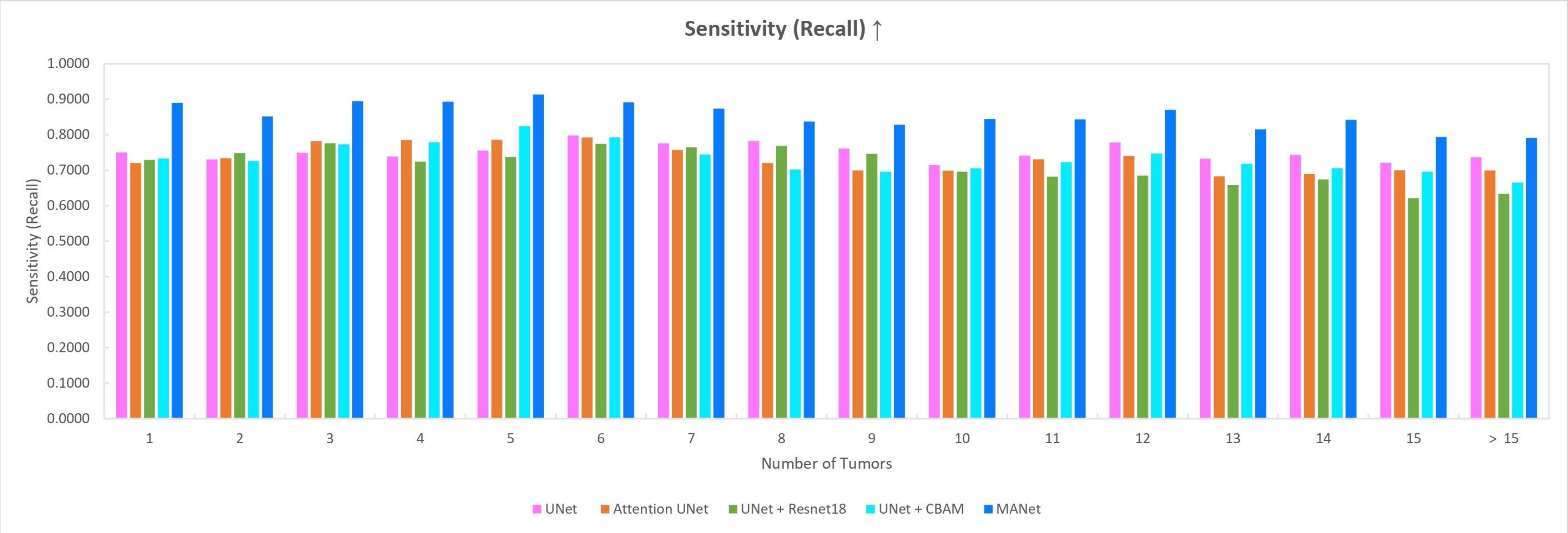

Quantitative Analysis based on the Number of Tumors

Average Symmetric Surface Distance (ASSD)

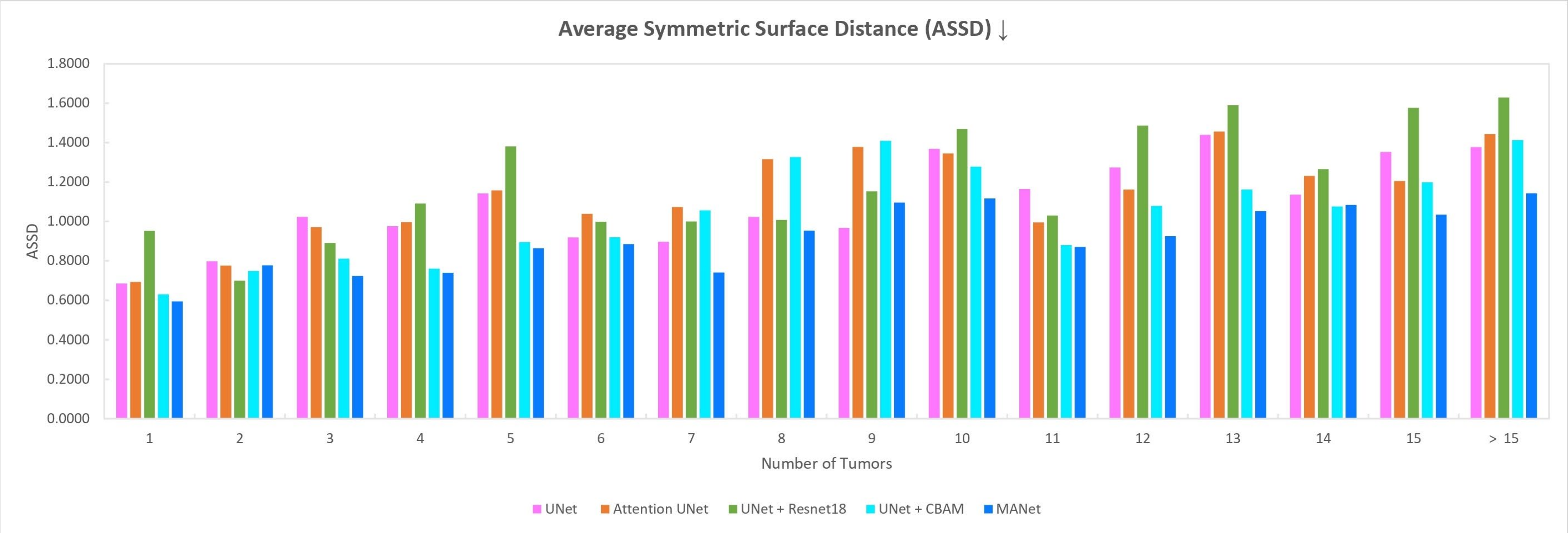

Quantitative Analysis based on the Number of Tumors

Volume Overlap Error (VOE)

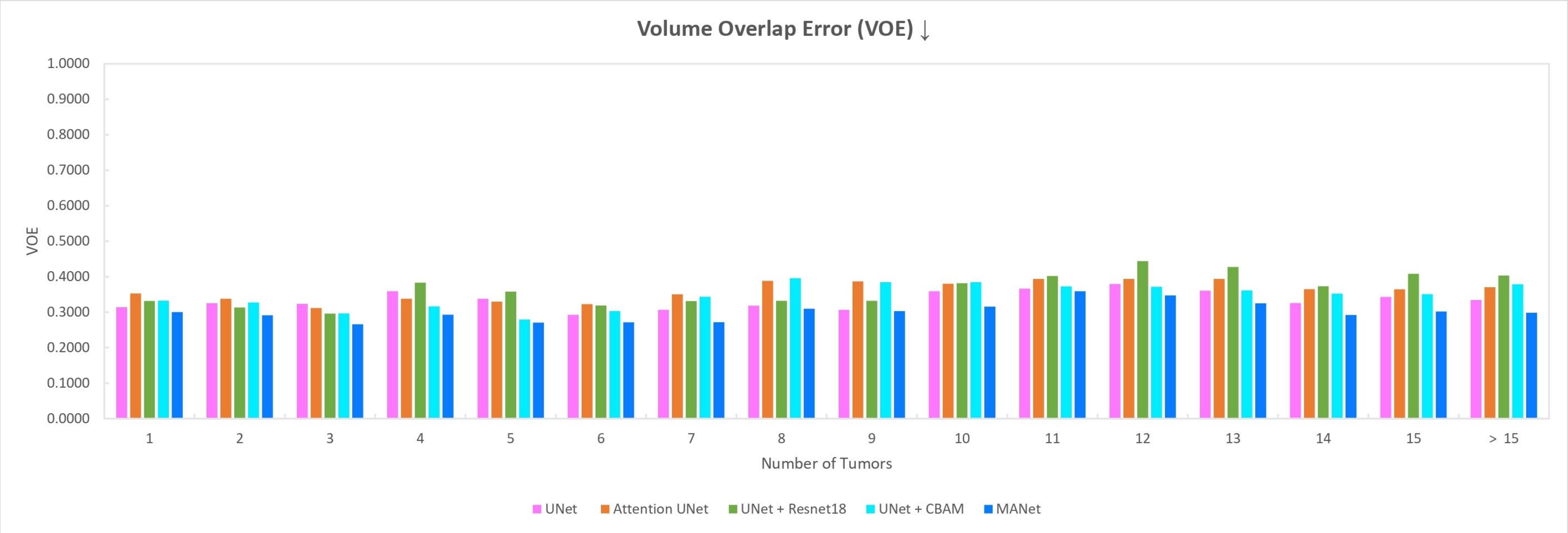

Quantitative Analysis based on the Number of Tumors

Specificity

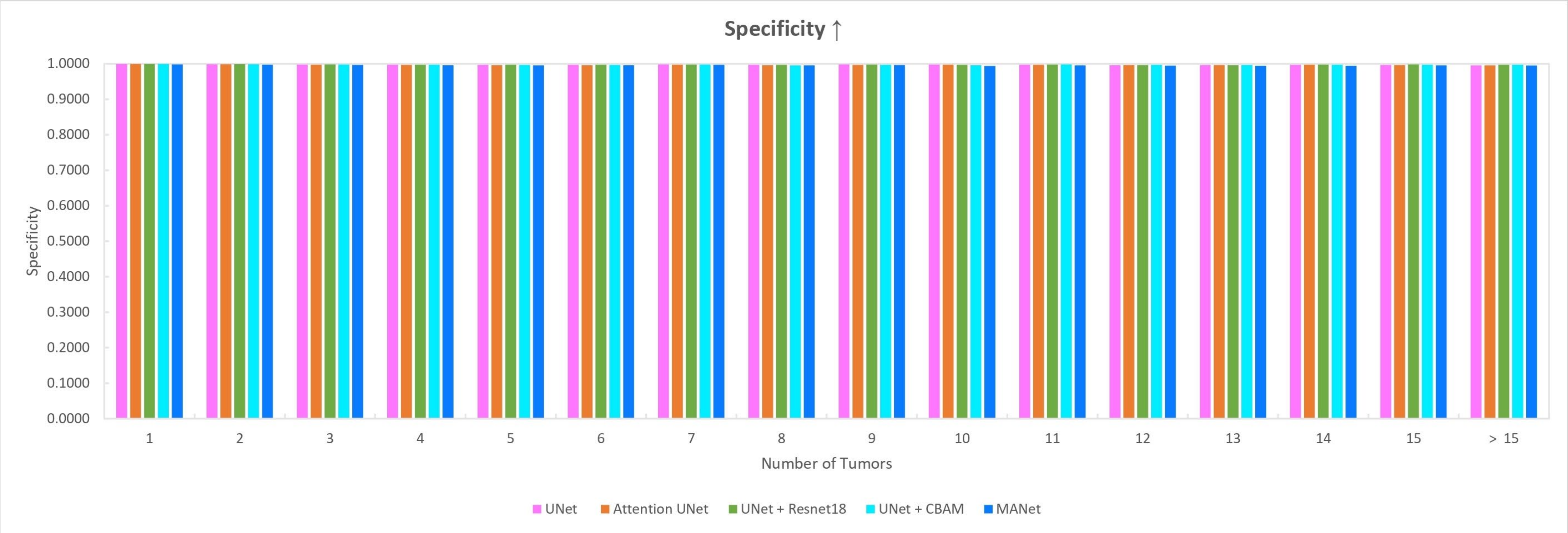

Quantitative Analysis based on the Number of Tumors

Accuracy

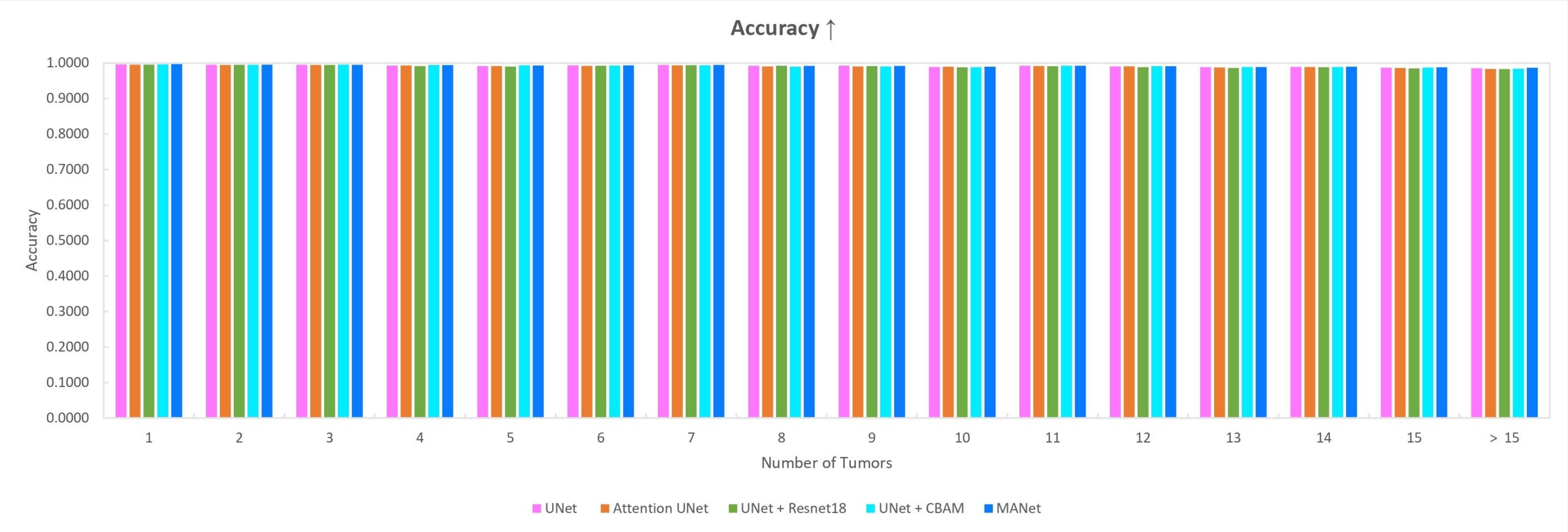

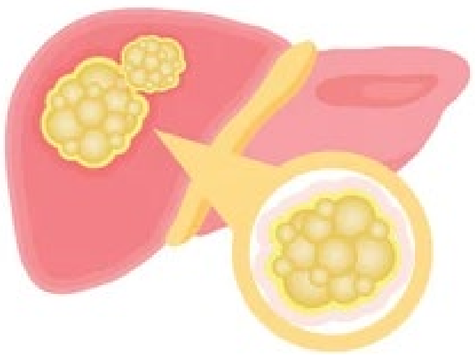

Quantitative Analysis based on the Total Area of Tumors

Quantitative Analysis based on the Total Area of Tumors

CT slice data distribution based on the total area of liver tumors

Total Tumor Area (mm^2)	Number of Slices
0 - 1000	410
1000 - 2000	212
2000 - 3000	154
3000 - 4000	174
4000 - 5000	182
5000 - 6000	100
6000 - 7000	58
7000 - 8000	74
8000 - 9000	42
9000 - 10000	4

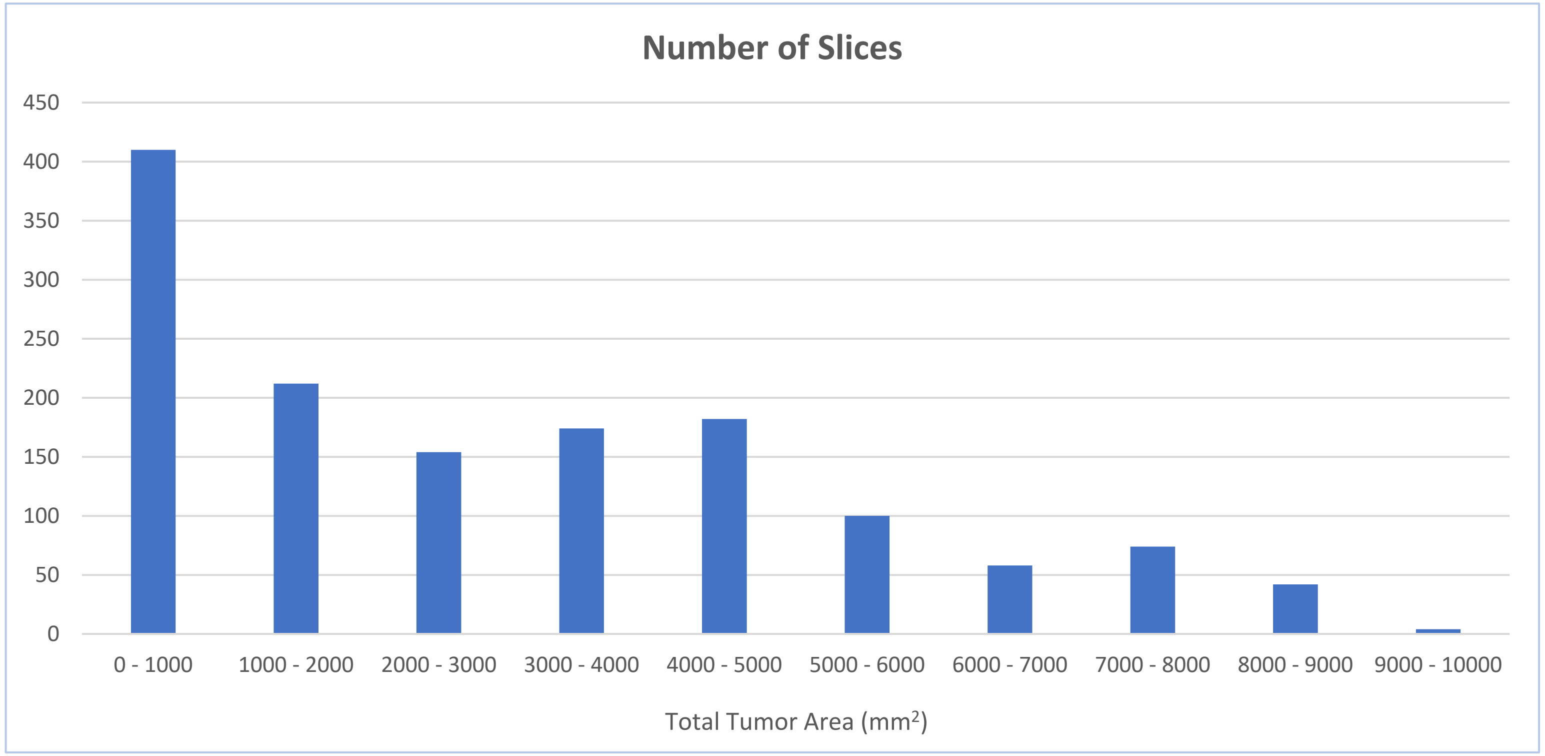

Quantitative Analysis based on the Total Area of Tumors

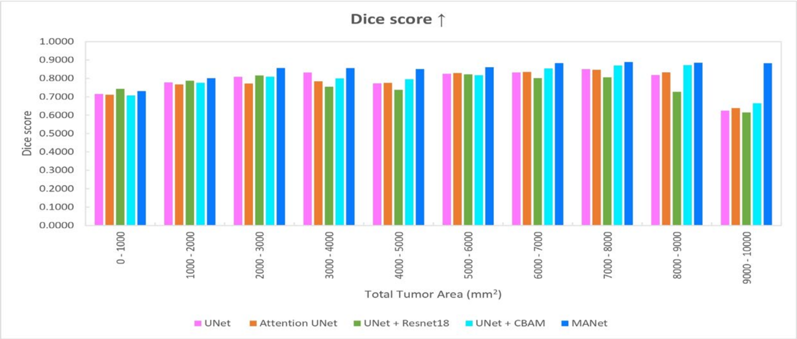

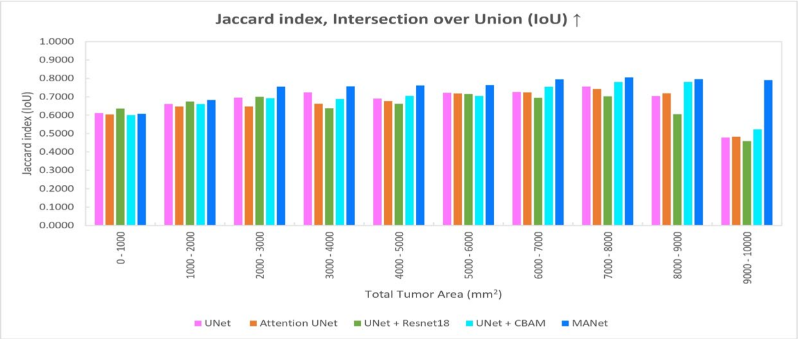

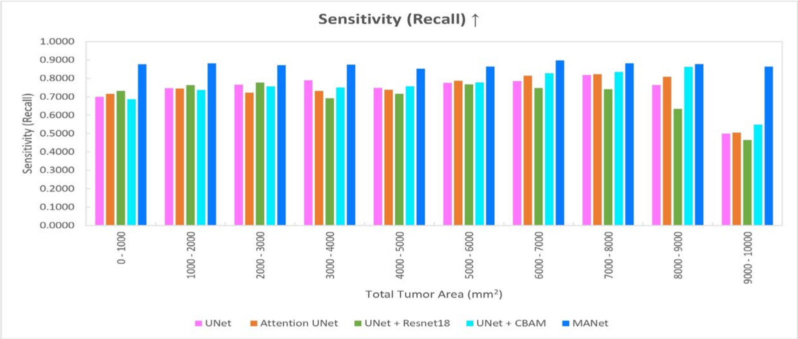

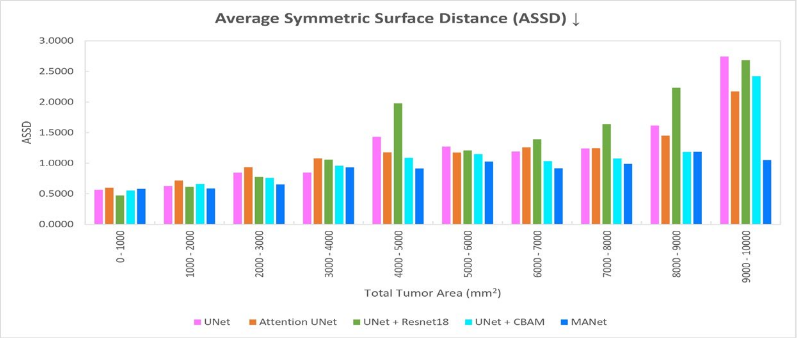

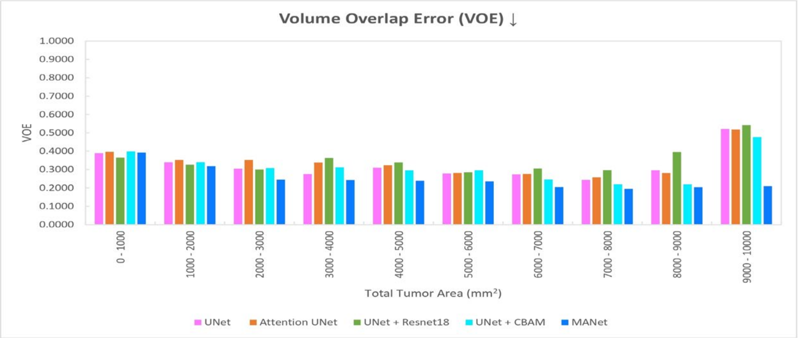

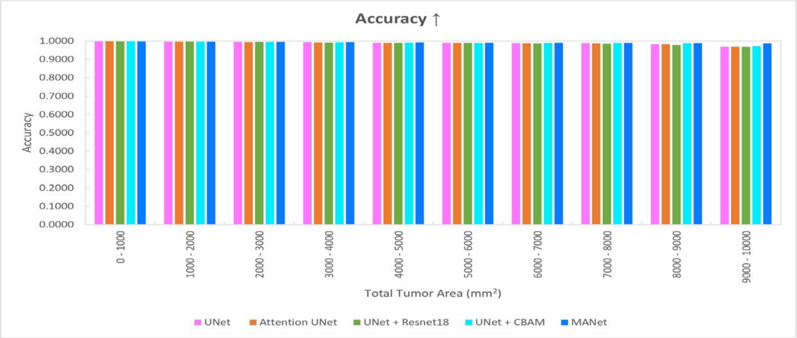

Quantitative Analysis based on the Total Area of Tumors

Dice score

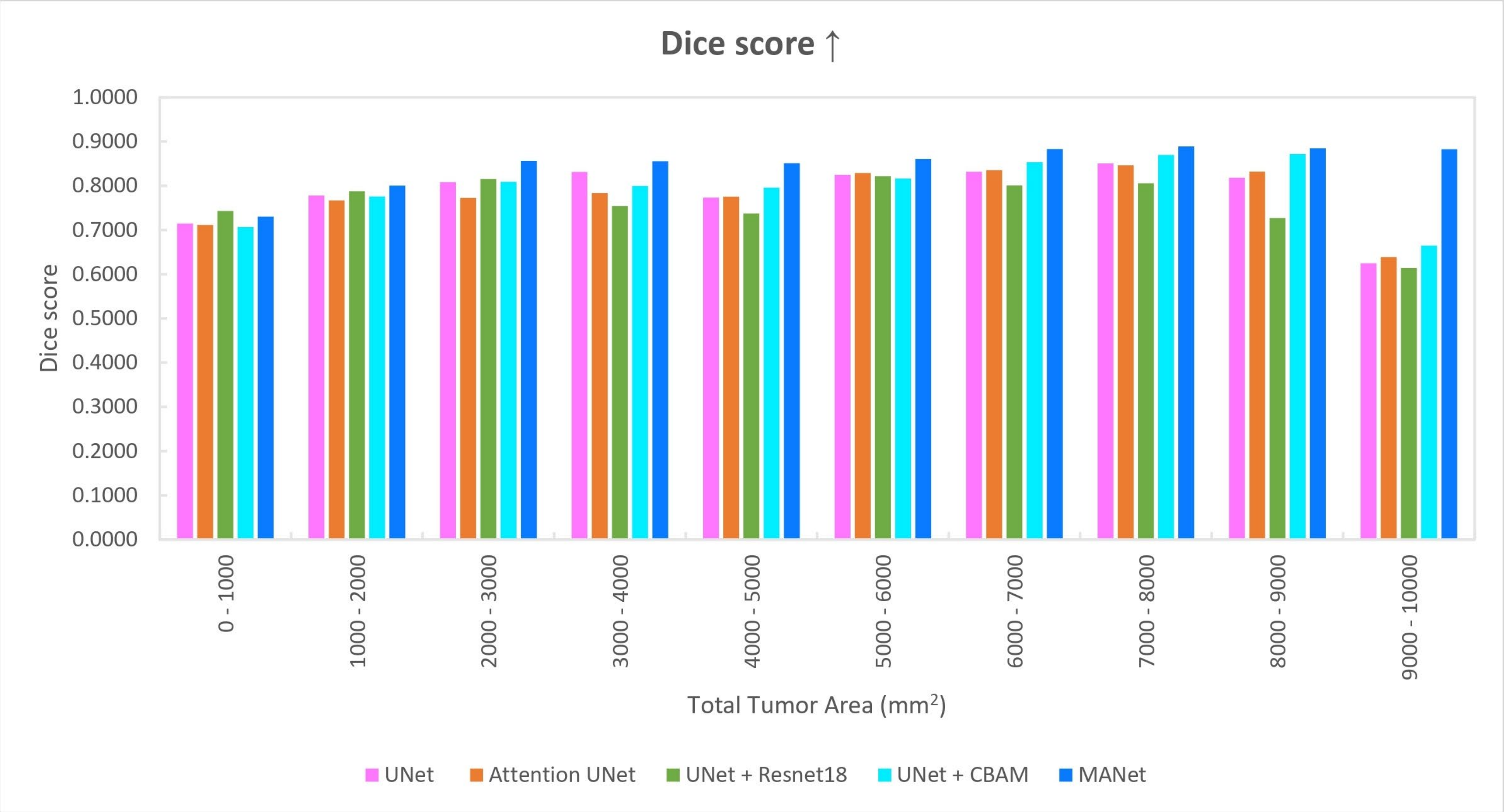

Quantitative Analysis based on the Total Area of Tumors

Jaccard index, Intersection over Union (IoU)

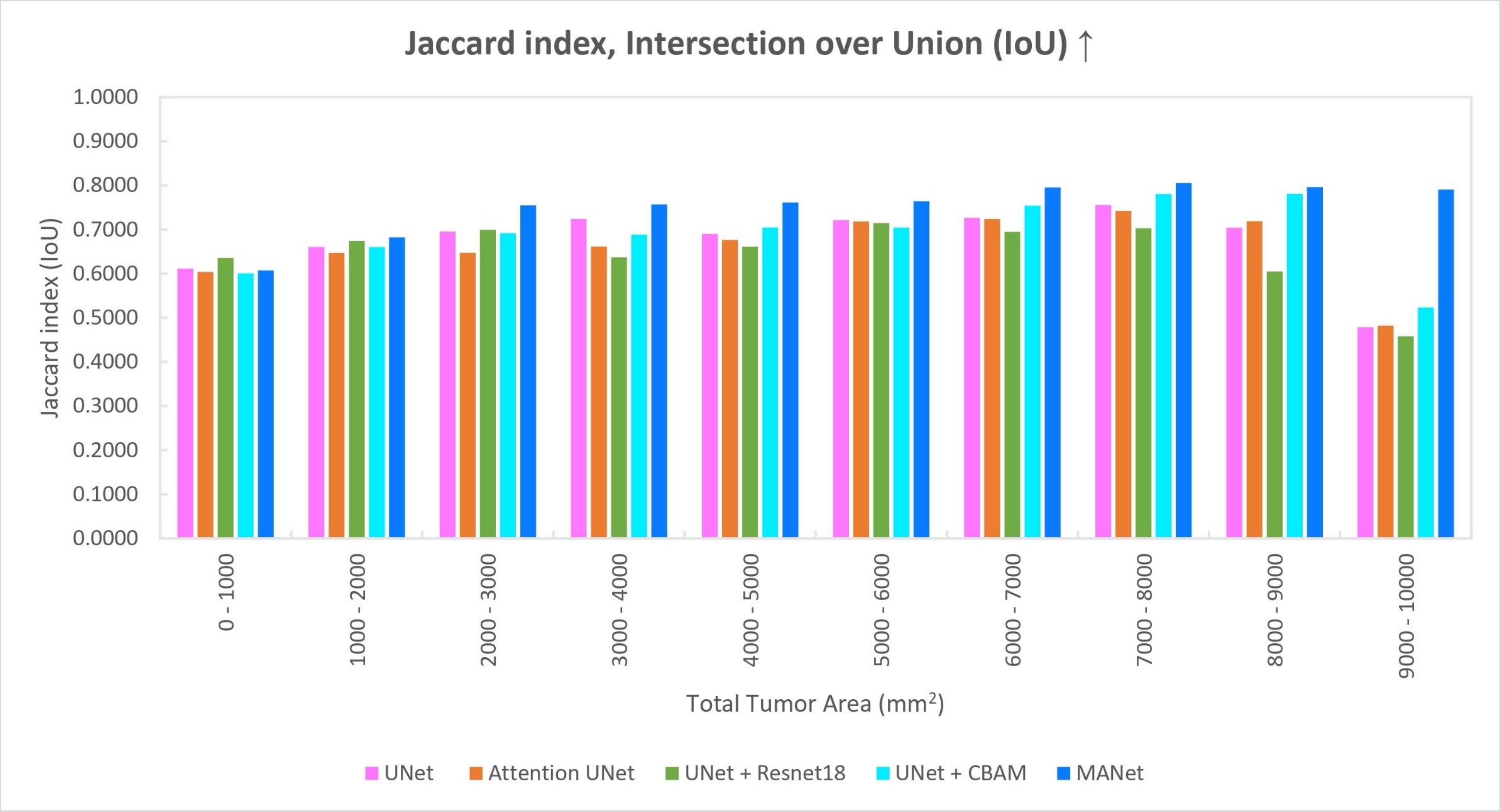

Quantitative Analysis based on the Total Area of Tumors

Sensitivity (Recall)

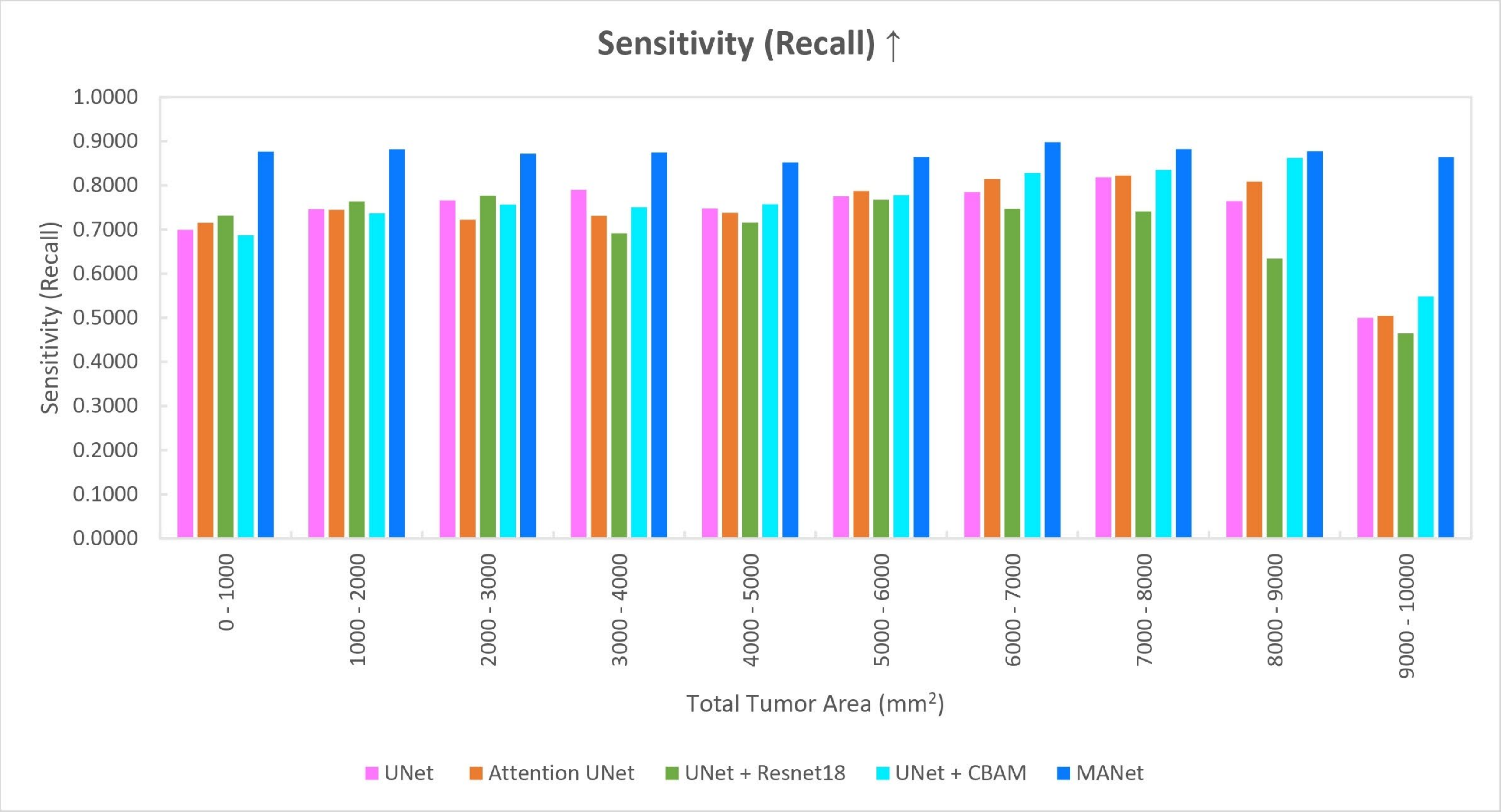

Quantitative Analysis based on the Total Area of Tumors

Average Symmetric Surface Distance (ASSD)

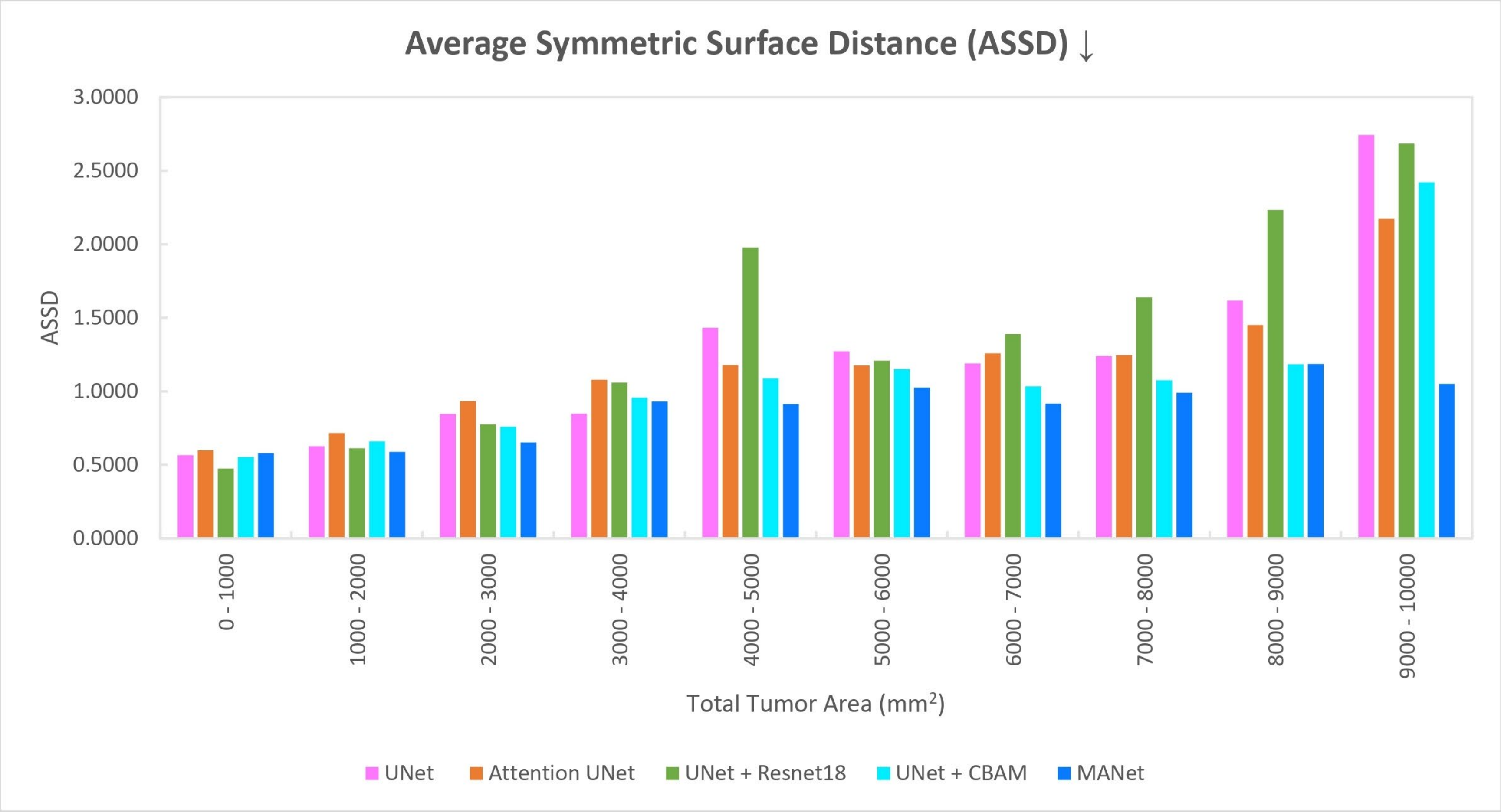

Quantitative Analysis based on the Total Area of Tumors

Volume Overlap Error (VOE)

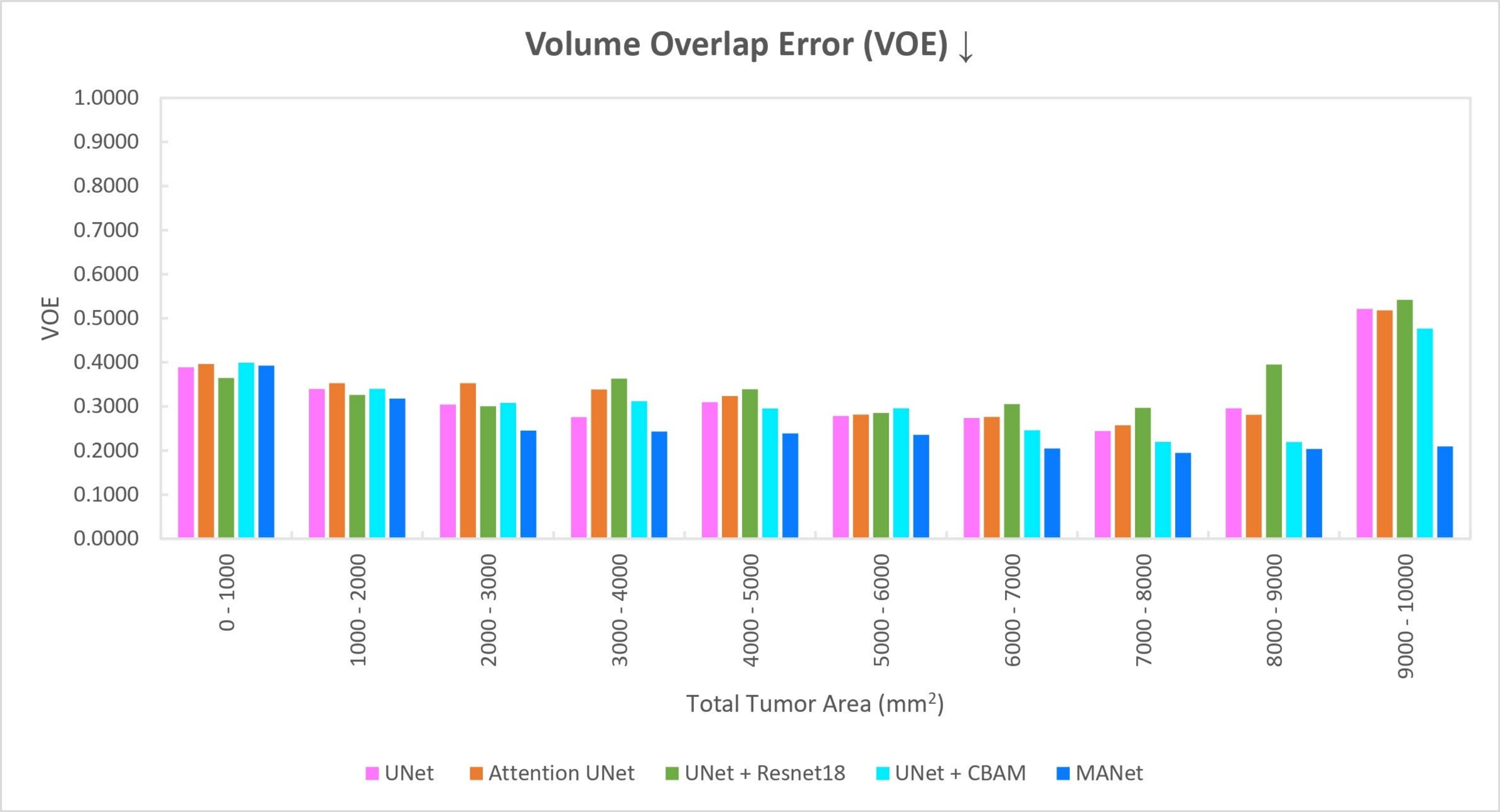

Quantitative Analysis based on the Total Area of Tumors

Specificity

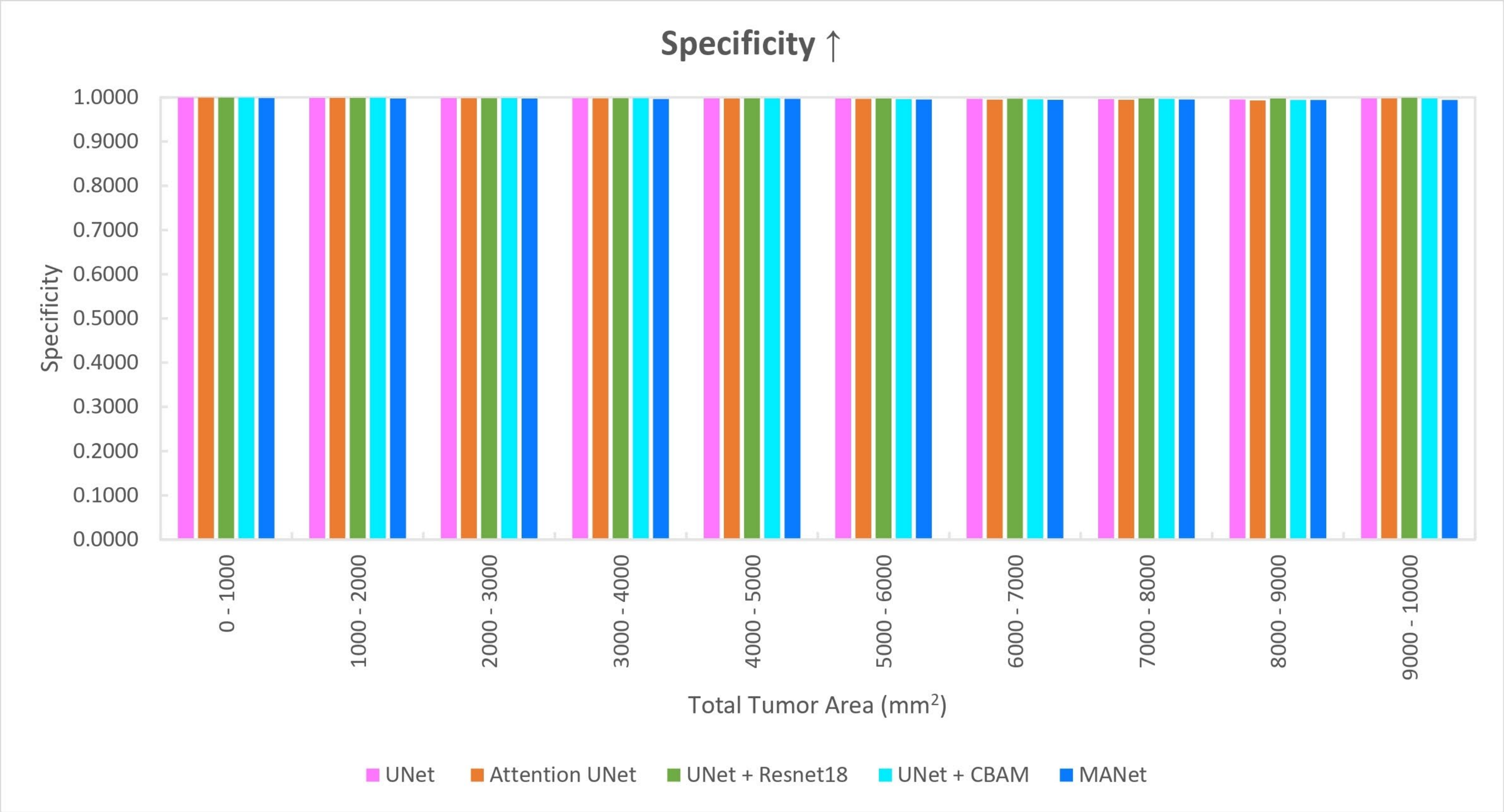

Quantitative Analysis based on the Total Area of Tumors

Accuracy

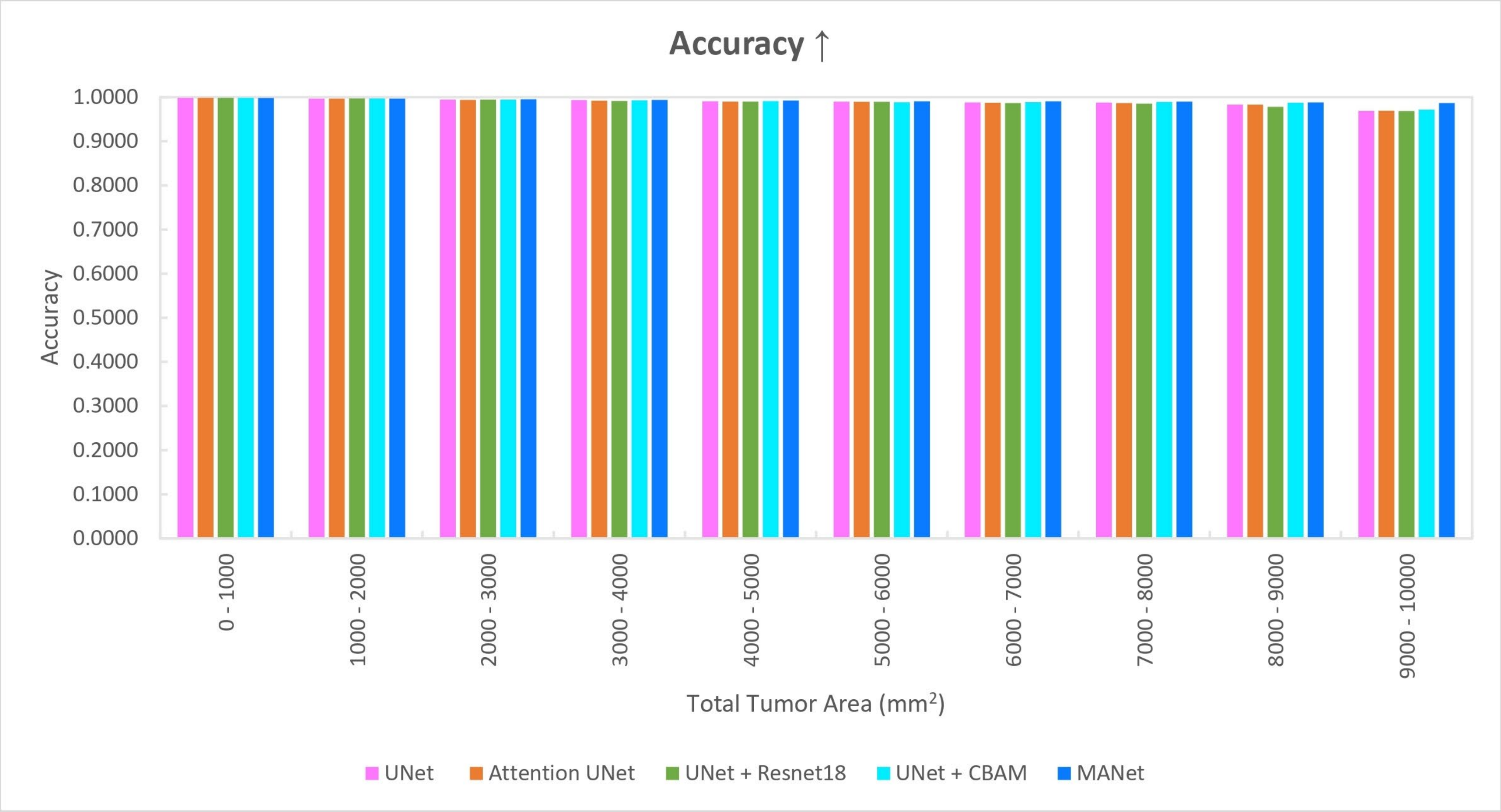

Liver Tumor Segmentation Validation with a Radiologist

Liver Tumor Segmentation Validation with a Radiologist

Validation sample	Remark of the Radiologist		
	Poor than UNet	Same as UNet	Better than UNet
Sample 1			√
Sample 2			√
Sample 3			√
Sample 4			√
Sample 5		√	
Sample 6			√
Sample 7	√		
Sample 8		√	
Sample 9			√
Sample 10			√
Sample 11		√	
Sample 12			√
Sample 13			√
Sample 14			√
Sample 15			√
Sample 16		√	
Sample 17		√	
Sample 18			√

Table 5.17: The remark of the radiologist for the liver tumor segmentation results validation.

Liver Tumor Segmentation Validation with a Radiologist

- Sample 5
- Sample 6
- Sample 7

Validation sample	Remark of the Radiologist		
	Poor than UNet	Same as UNet	Better than UNet
Sample 1			√
Sample 2			√
Sample 3			√
Sample 4			√
Sample 5		√	
Sample 6			√
Sample 7	√		
Sample 8		√	
Sample 9			√
Sample 10			√
Sample 11		√	
Sample 12			√
Sample 13			√
Sample 14			√
Sample 15			√
Sample 16		√	
Sample 17		√	
Sample 18			√

Table 5.17: The remark of the radiologist for the liver tumor segmentation results validation.

Liver Tumor Segmentation Validation with a Radiologist

Sample 6

Better than UNet

Image	Ground Truth	Prediction: UNet	Prediction: Proposed Model

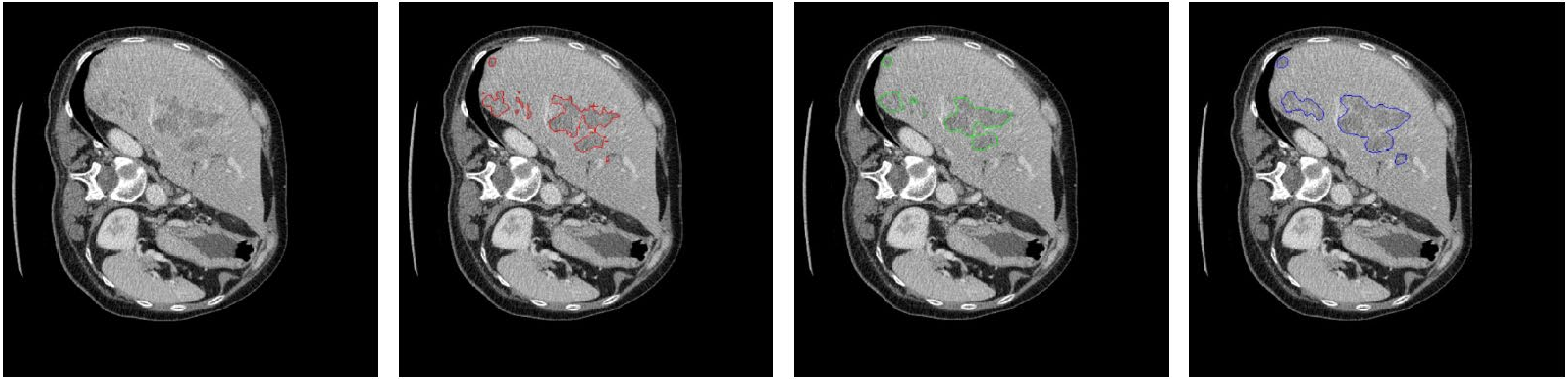

		DSC: 0.8560	DSC: 0.7623

Comment of the radiologist: The ground truth does not include all the areas of the tumor. And the UNet has followed the ground truth. The proposed model has recognized all the tumor regions even better than the ground truth.

Liver Tumor Segmentation Validation with a Radiologist

Sample 5

Same as UNet

Image	Ground Truth	Prediction: UNet	Prediction: Proposed Model

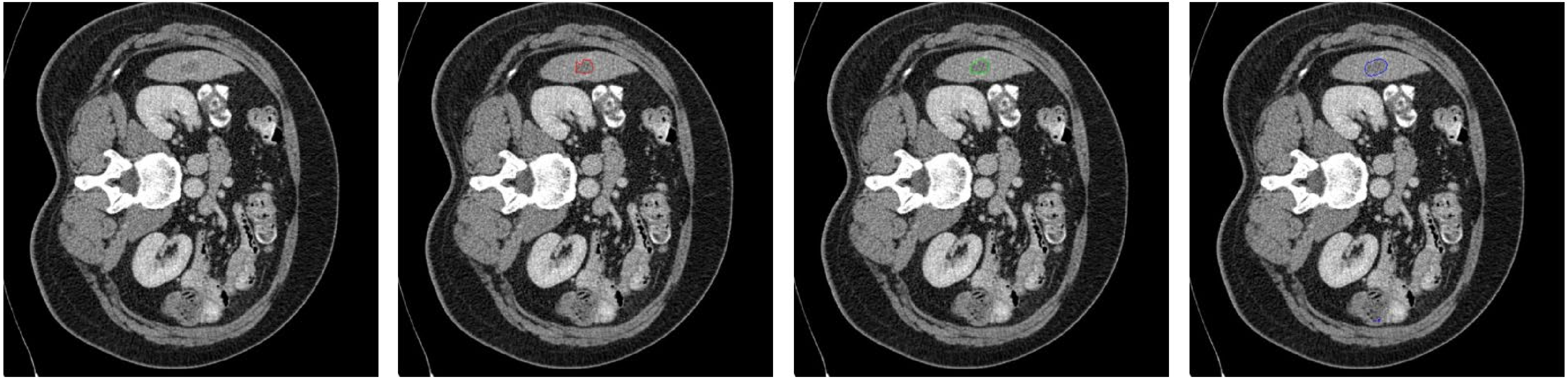

		DSC: 0.9098	DSC: 0.7966

Comment of the radiologist: Both segmentations are acceptable. There is no significant difference in segmentations of UNet and proposed model. However, proposed model has included fuzzy tumor boundary to the segmentation mask.

Liver Tumor Segmentation Validation with a Radiologist

Sample 7

Poor than UNet

Image	Ground Truth	Prediction: UNet	Prediction: Proposed Model

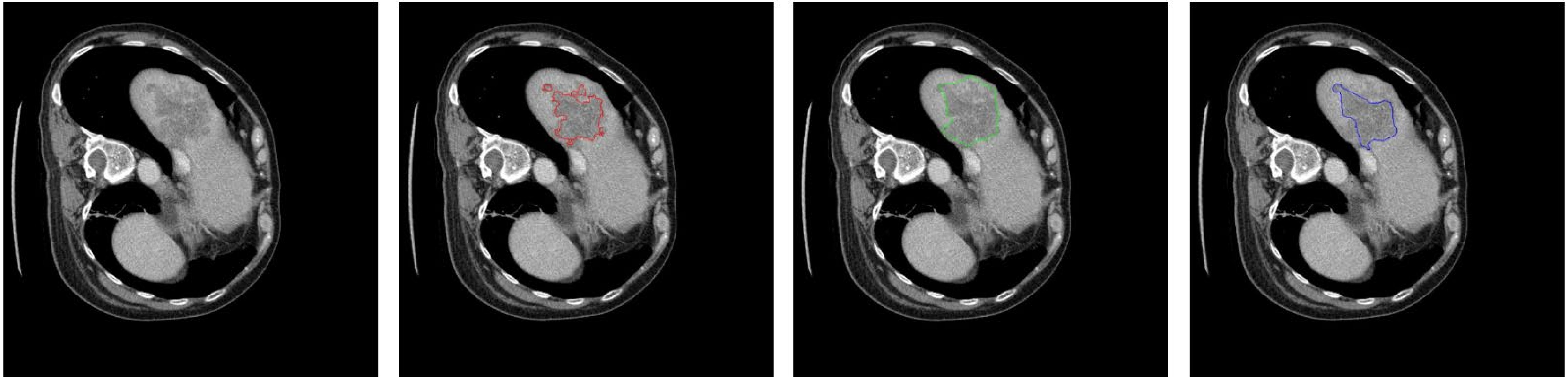

		DSC: 0.7775	DSC: 0.8069

Comment of the radiologist: The ground truth does not cover the whole tumor region. The proposed model has partially segmented the tumor region. However, the UNet has segmented the whole area of the tumor.

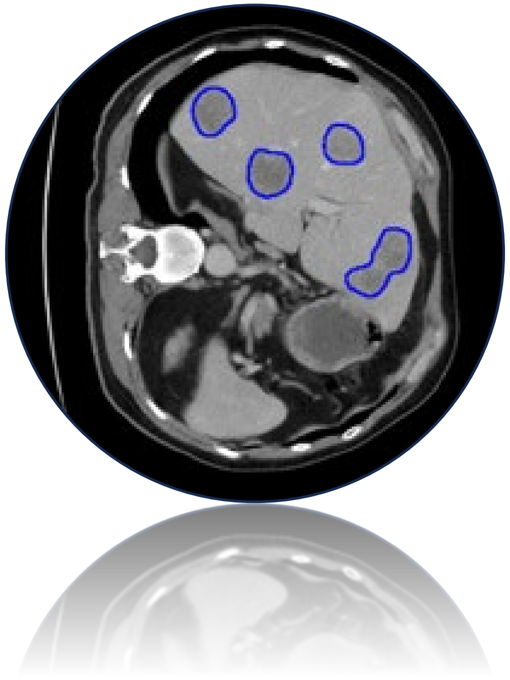

Qualitative Analysis of Segmentation Mask

Qualitative Analysis of Segmentation Mask

The qualitative analysis of liver tumor segmentation performance from the slice-based segmentation experiment

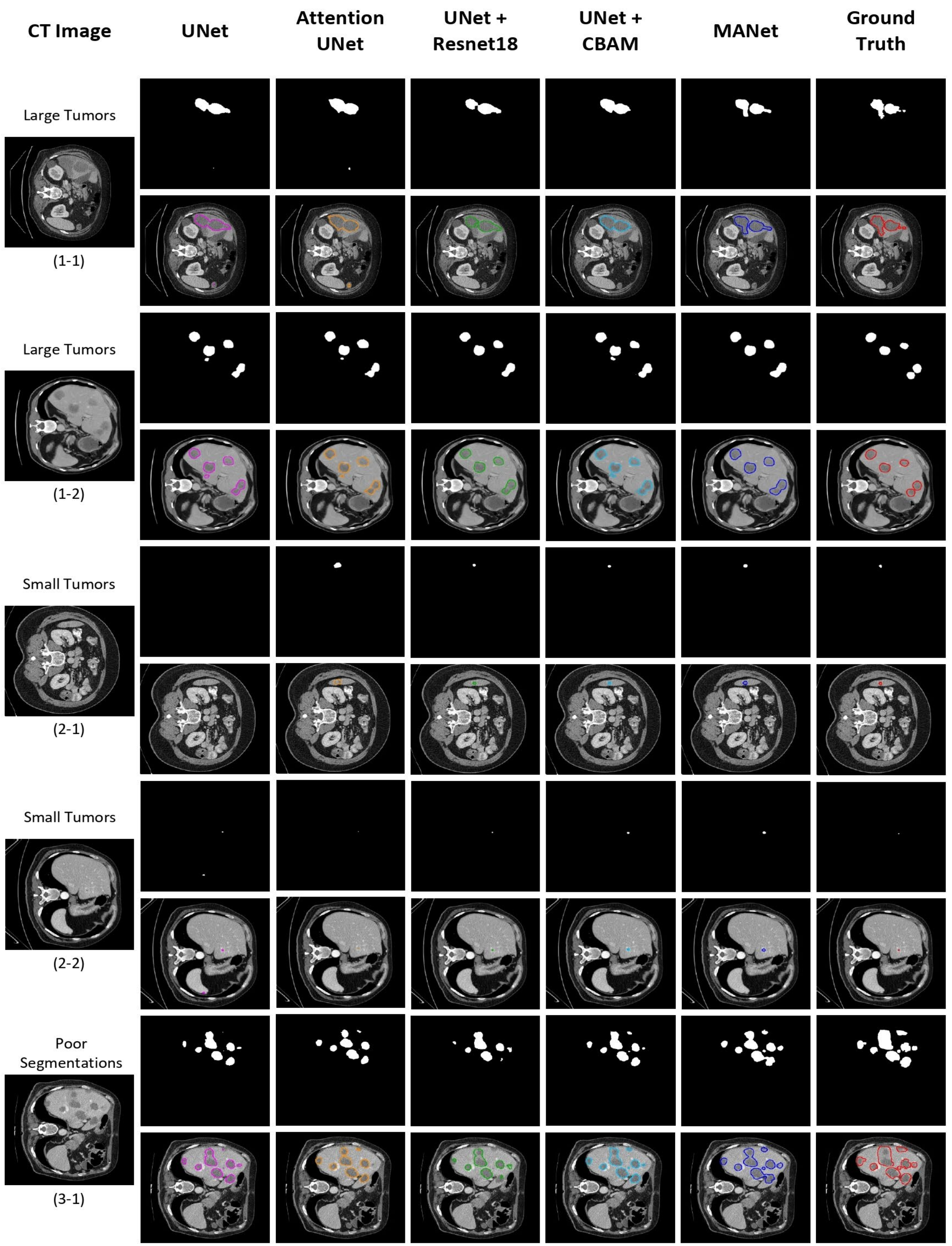

Qualitative Analysis of Segmentation Mask

The qualitative analysis of liver tumor segmentation performance from the slice-based segmentation experiment

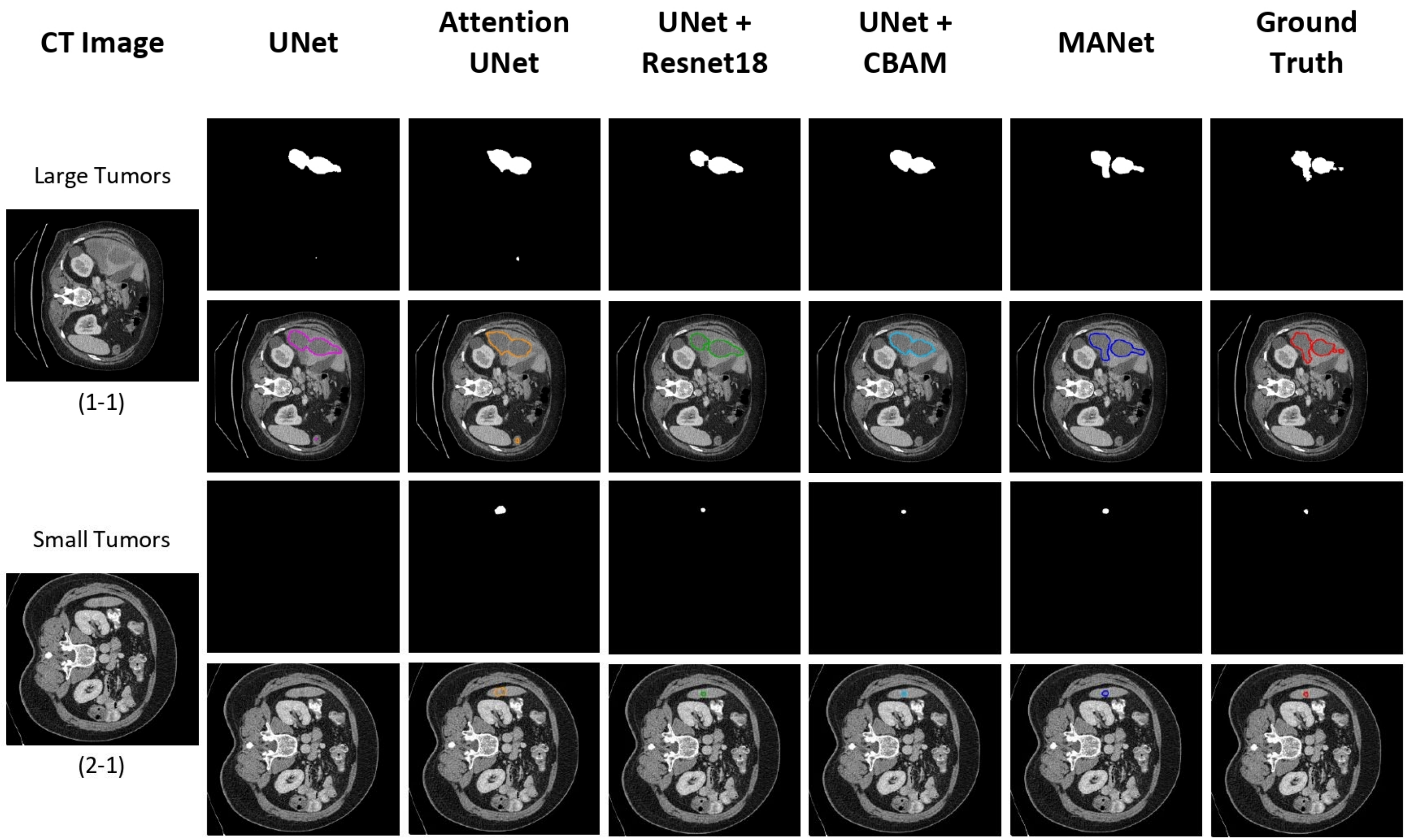

Qualitative Analysis of Segmentation Mask

The qualitative analysis of liver tumor segmentation performance from the volume-based segmentation experiment

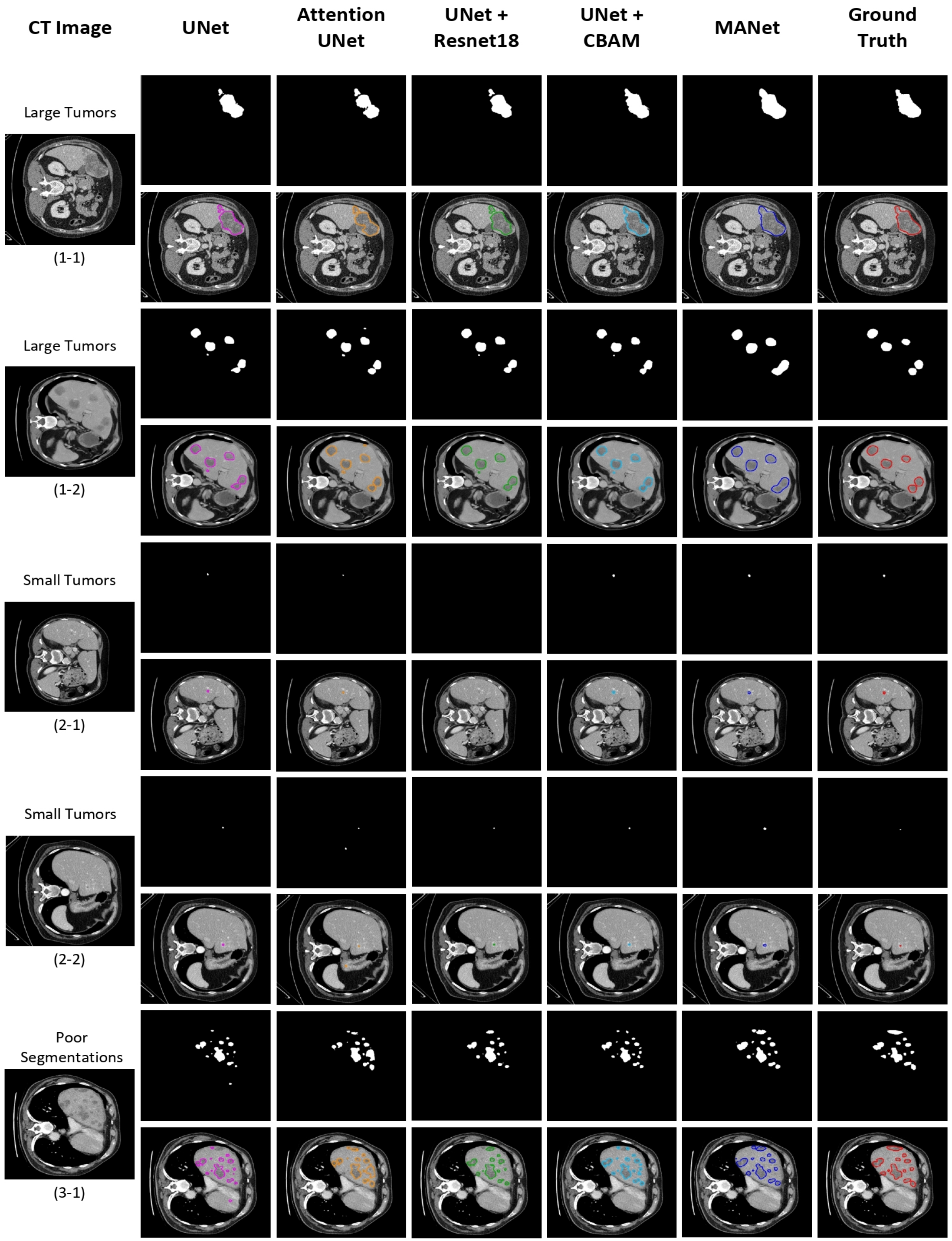

Qualitative Analysis of Segmentation Mask

The qualitative analysis of liver tumor segmentation performance from the volume-based segmentation experiment

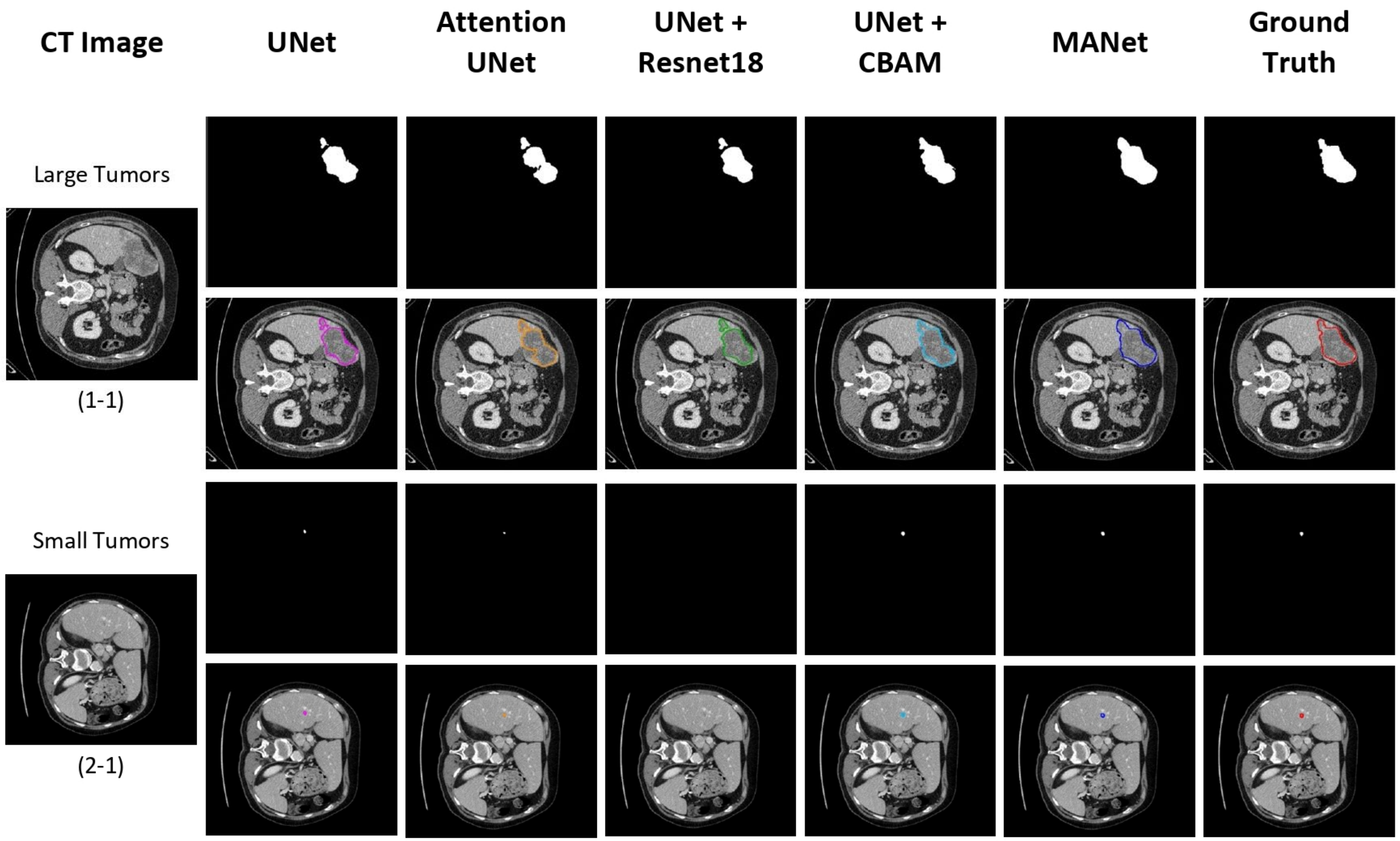

Qualitative Analysis of Segmentation Mask

Liver tumor segmentation performance comparison: Slice-based vs Volume-based

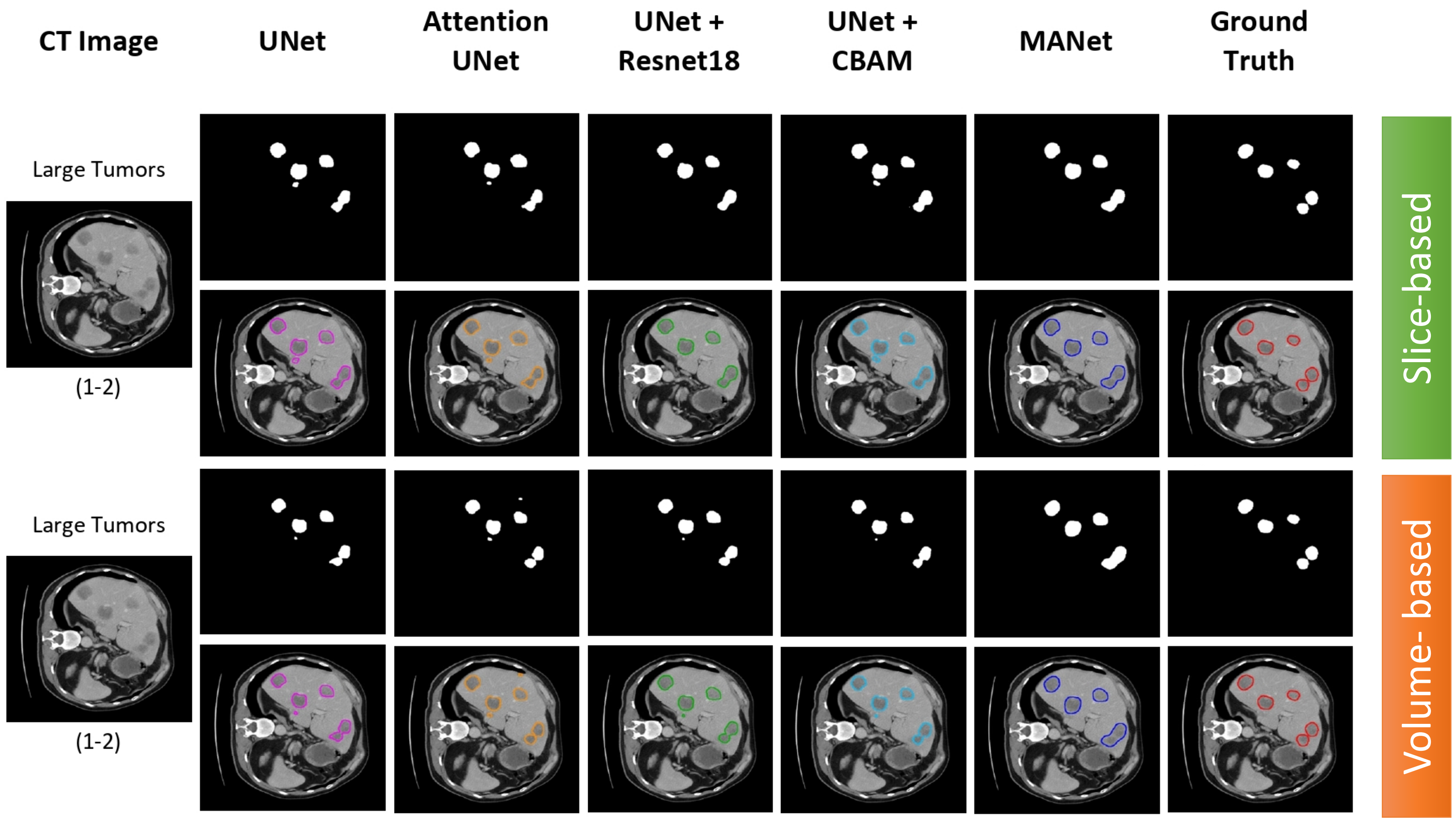

Qualitative Analysis of Segmentation Mask

Liver tumor segmentation performance comparison: Slice-based vs Volume-based

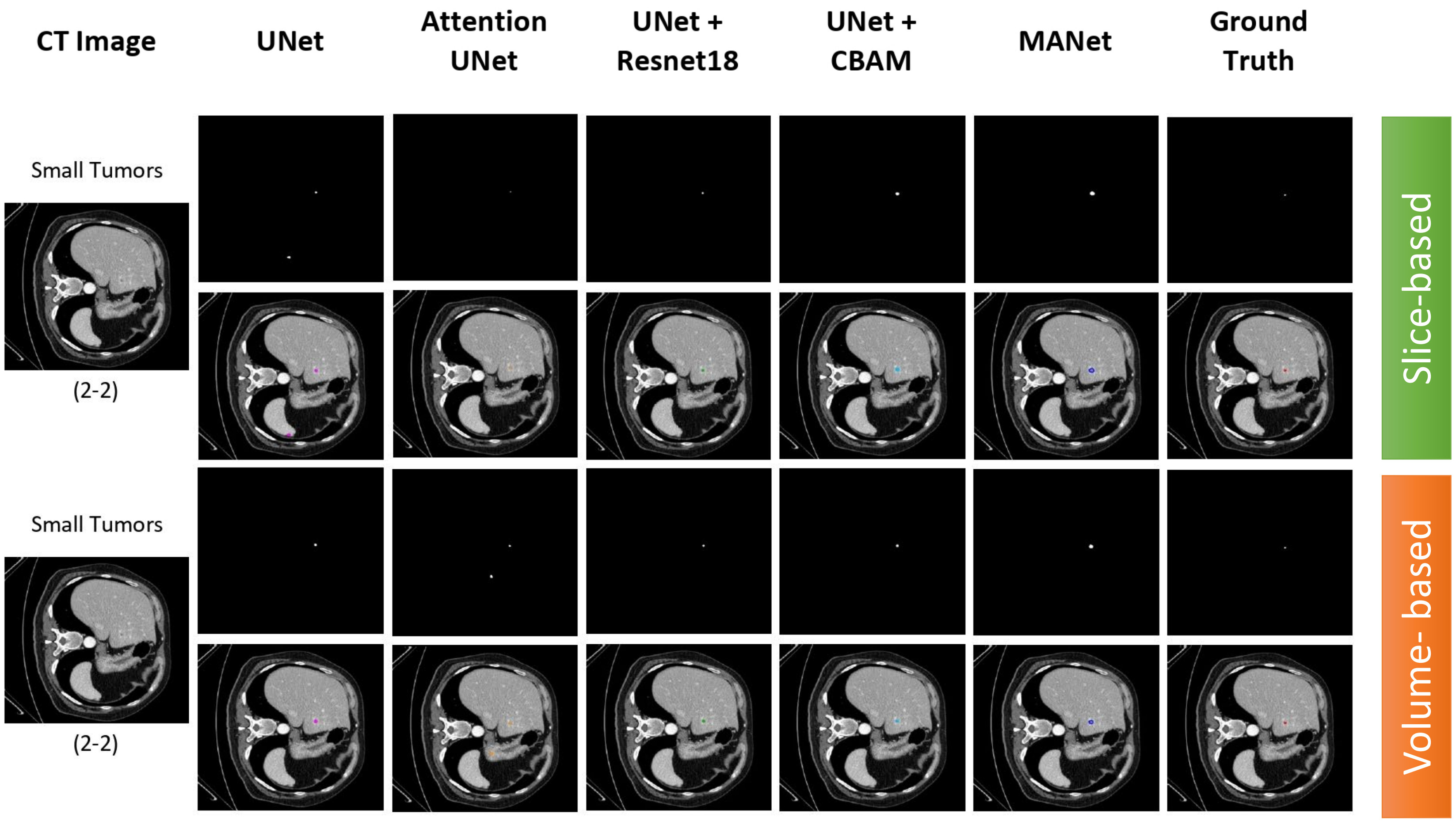

Qualitative Analysis of Segmentation Mask

Liver tumor segmentation performance comparison: Slice-based vs Volume-based

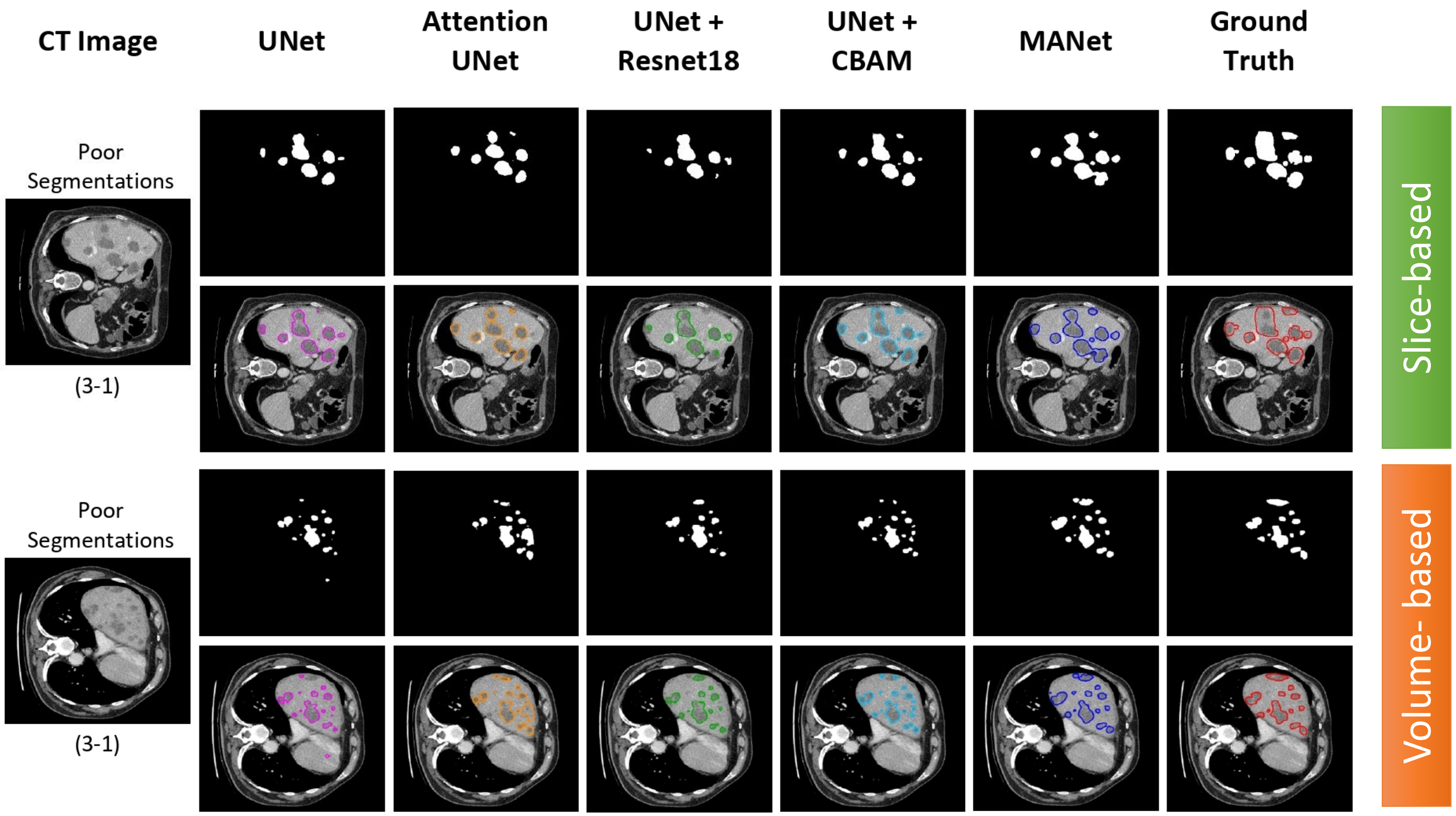

Qualitative Analysis of Segmentation Mask

The qualitative analysis of liver tumor segmentation performance in over/non-segmentations in multiple tumor cases from the slice-based segmentation experiment

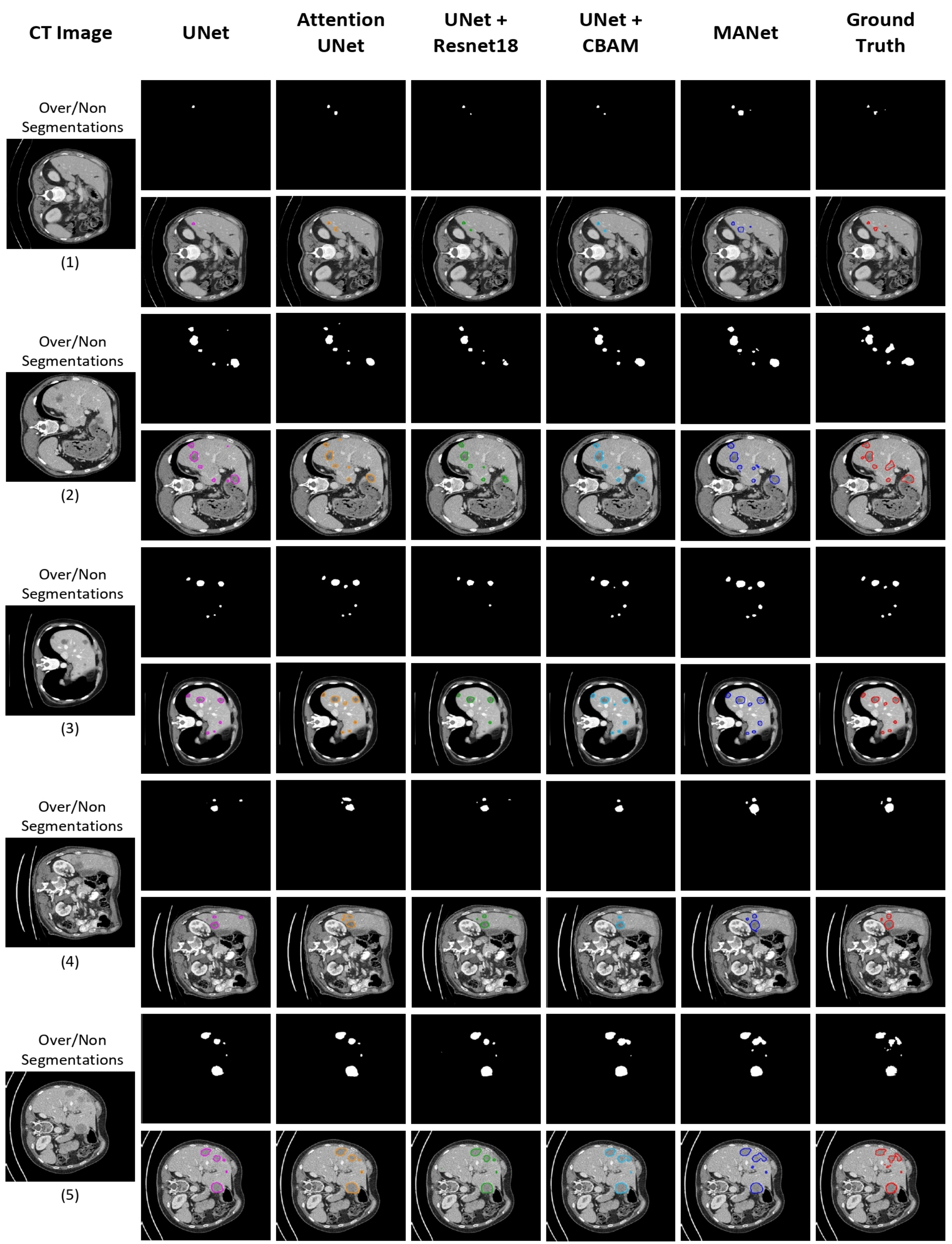

Qualitative Analysis of Segmentation Mask

The qualitative analysis of liver tumor segmentation performance of the **proposed MANet model and state-of-the-art models** from the slice-based segmentation experiment

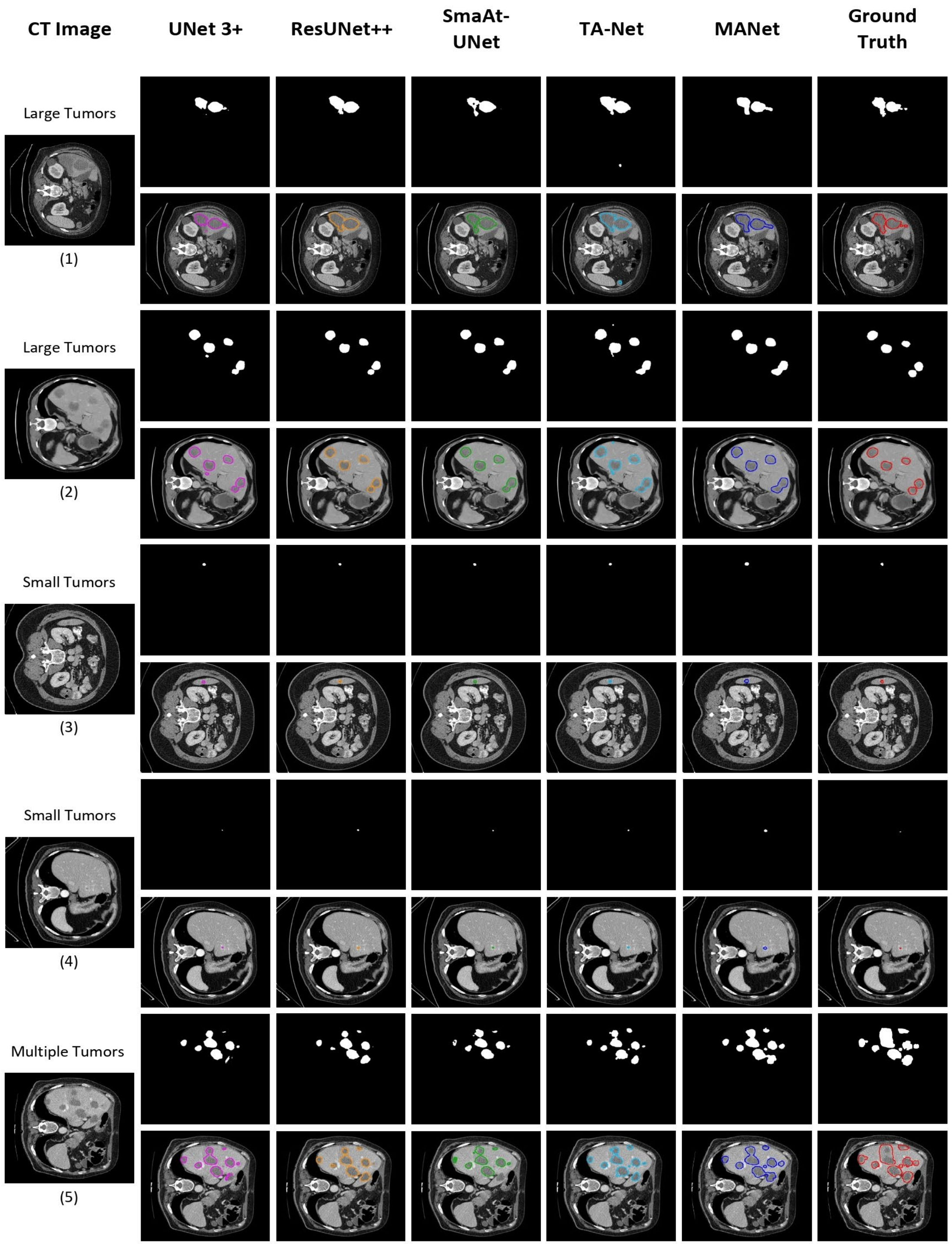

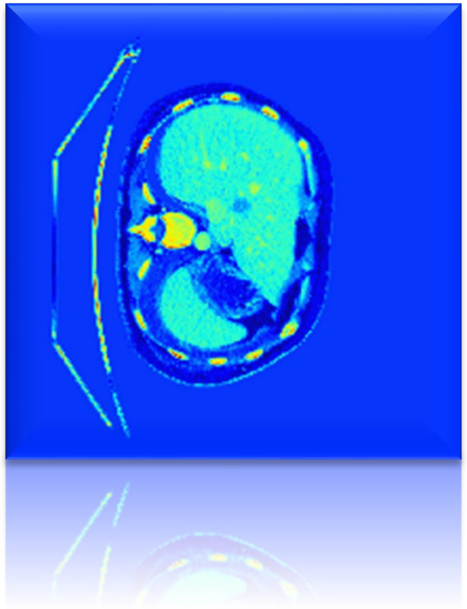

Model Feature Visualization

Model Feature Visualization

Feature visualization of MANet architecture

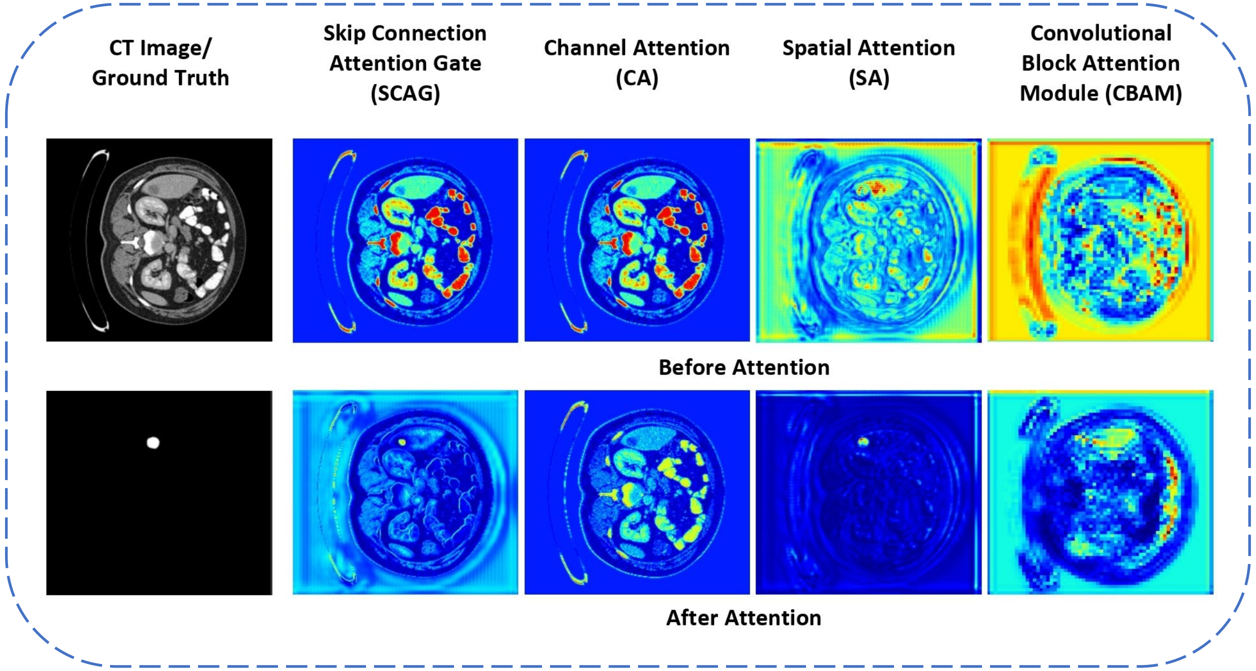

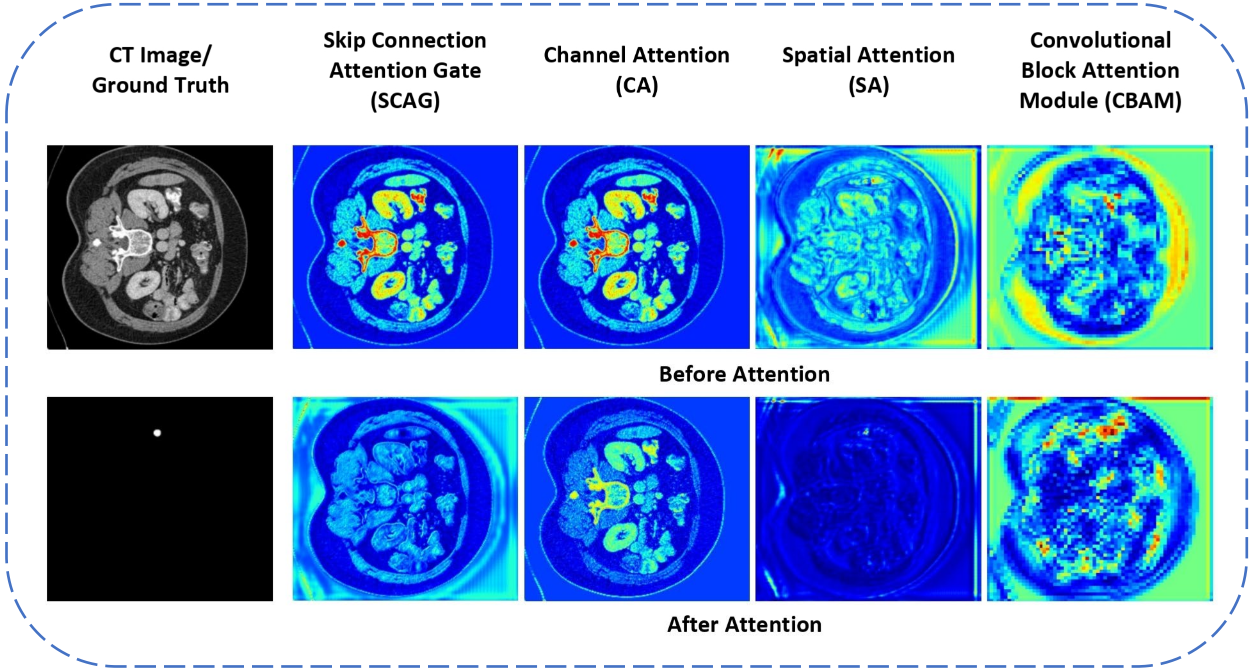

Model Feature Visualization

Feature visualization of MANet architecture and comparison networks

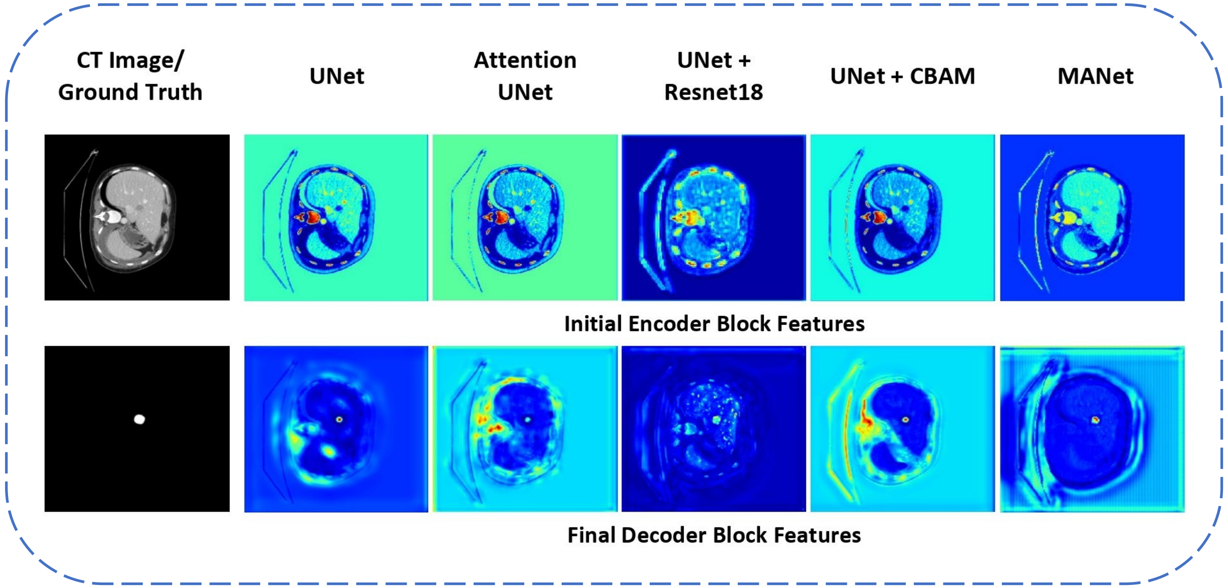

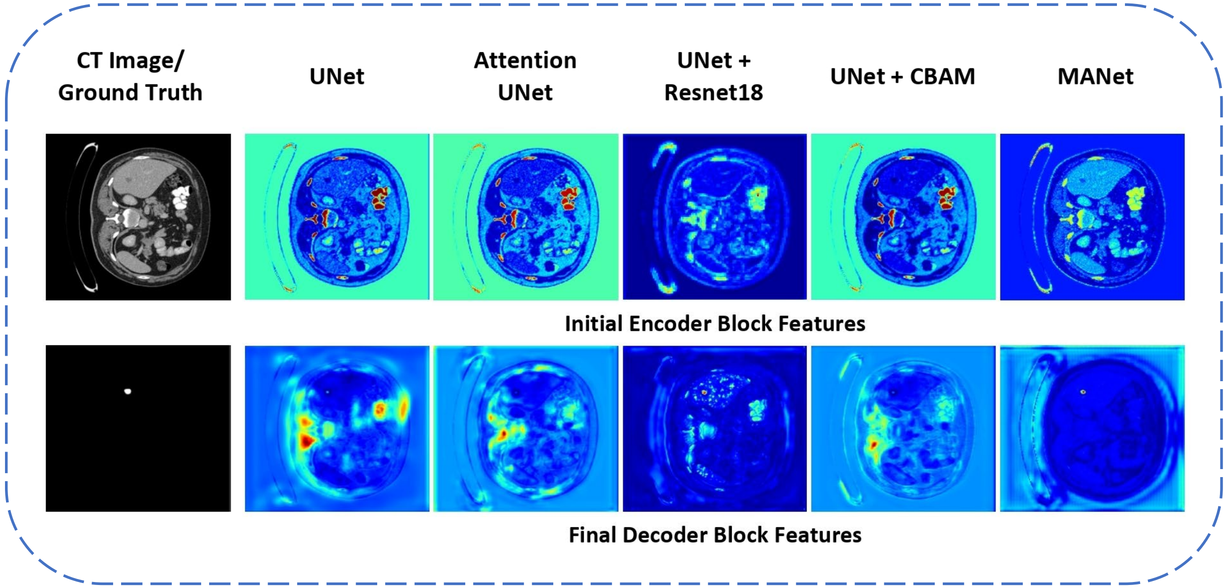

Computational Cost Analysis

Computational Cost Analysis

Network	Computational complexity (MACs(G))	Total training parameters (M)	Inference time (ms)
UNet	**94.45**	13.37	41.60
Attention UNet	97.07	**6.34**	38.80
UNet + Resnet18	119.14	17.85	**36.20**
UNet + CBAM	166.80	8.39	82.60
MANet (Proposed model)	132.37	7.83	81.80

Table 5.18: Analysis of computational costs based on computational complexity, total training parameters, and inference time. The best values are in bold

Ablation Analysis

Ablation Analysis

No	Method	Dice score	ASSD	Jaccard index (IoU)	VOE	Accuracy	Sensitivity (Recall)	Specificity
1	UNet	0.7522 ± 0.178	1.4342 ± 1.320	0.6310 ± 0.190	0.3606 ± 0.190	0.9928 ± 0.006	0.8425 ± 0.204	0.9956 ± 0.003
2	UNet + RB	0.7533 ± 0.182	1.5172 ± 1.395	0.6359 ± 0.192	0.3640 ± 0.192	0.9925 ± 0.006	0.8512 ± 0.202	0.9951 ± 0.004
3	UNet + RB + SCAG	0.7532 ± 0.195	1.4247 ± 1.298	0.6353 ± 0.202	0.3646 ± 0.202	0.9927 ± 0.006	0.8329 ± 0.224	0.9956 ± 0.003
4	UNet + RB + CA	0.8010 ± 0.155	1.0137 ± 1.000	0.6901 ± 0.177	0.3027 ± 0.177	0.9940 ± **0.004**	0.8708 ± 0.173	0.9965 ± **0.002**
5	UNet + RB + SA	0.7550 ± 0.201	1.1610 ± 1.069	0.6389 ± 0.205	0.3610 ± 0.205	0.9929 ± 0.006	0.8292 ± 0.233	0.9958 ± 0.003
6	UNet + RB + CBAM	0.8006 ± 0.157	0.8842 ± 0.814	0.6897 ± 0.178	0.3038 ± 0.178	0.9938 ± **0.004**	0.8712 ± 0.180	0.9962 ± 0.003
7	UNet + SCAG + CA + SA + CBAM	0.8056 ± 0.153	0.8376 ± 0.733	0.6992 ± 0.174	0.3007 ± 0.174	0.9941 ± **0.004**	0.8715 ± 0.177	0.9967 ± 0.003
8	**MANet: UNet + RB + SCAG + CA + SA + CBAM**	**0.8145 ± 0.150**	**0.7084 ± 0.701**	**0.7084 ± 0.171**	**0.2915 ± 0.171**	**0.9947 ± 0.004**	**0.8723 ± 0.173**	**0.9970 ± 0.002**

Table 5.19: Ablation analysis for the proposed MANet architecture. The result from MANet and the best values are in bold.

RB: Residual Block
SCAG: Skip Connection Attention Gate
CA: Channel Attention
SA: Spatial Attention
CBAM: Convolutional Block Attention Module

05 Conclusion

Conclusion

01 The proposed methods is demonstrated a performance boost in liver tumor segmentation compared to the baseline methods.

02 Attention mechanisms effectively minimize computational costs while improving the segmentation performance.

03 The proposed model demonstrated better robustness and generalizability by performing well in both datasets and all the experiments.

Future Direction

- Analyze the effectiveness of the model to segment the liver and other organs with tumors (i.e., kidney, renal tumors)

- Experiment the applicability of the network with other radiological imaging modalities such as MRI, PET, and US

- Further optimize the architecture using state-of-the-art deep learning approaches to reduce computational complexity while improving the segmentation performance

Journal Article

MANet: a multi-attention network for automatic liver tumor segmentation in computed tomography (CT) imaging

scientific reports

OPEN

MANet: a multi-attention network for automatic liver tumor segmentation in computed tomography (CT) imaging

Kasun Hettihewa[1], Thananop Kobchaisawat[2], Natthaporn Tanpowpong[3] & Thanarat H. Chalidabhongse[1,4]✉

Automatic liver tumor segmentation is a paramount important application for liver tumor diagnosis and treatment planning. However, it has become a highly challenging task due to the heterogeneity of the tumor shape and intensity variation. Automatic liver tumor segmentation is capable to establish the diagnostic standard to provide relevant radiological information to all levels of expertise. Recently, deep convolutional neural networks have demonstrated superiority in feature extraction and learning in medical image segmentation. However, multi-layer dense feature stacks make the model quite inconsistent in imitating visual attention and awareness of radiological expertise for tumor recognition and segmentation task. To bridge that visual attention capability, attention mechanisms have developed for better feature selection. In this paper, we propose a novel network named Multi Attention Network (MANet) as a fusion of attention mechanisms to learn highlighting important features while suppressing irrelevant features for the tumor segmentation task. The proposed deep learning network has followed U-Net as the basic architecture. Moreover, residual mechanism is implemented in the encoder. Convolutional block attention module has split into channel attention and spatial attention modules to implement in encoder and decoder of the proposed architecture. The attention mechanism in Attention U-Net is integrated to extract low-level features to combine with high-level ones. The developed deep learning architecture is trained and evaluated on the publicly available MICCAI 2017 Liver Tumor Segmentation dataset and 3DIRCADb dataset under various evaluation metrics. MANet demonstrated promising results compared to state-of-the-art methods with comparatively small parameter overhead.

Liver cancer is one of the major cancer types with the most fatalities recorded around the world[1,2]. For immediate clinical management to be successful in achieving survival, early detection of liver tumors is essential. Tumor burden analysis which consists of major factors of measuring the size and location of the tumor, utmost importance to determine the severity of the disease. Medical imaging is a noninvasive technique to determine the severity and stratification of cancer. Radiologists mostly rely on Computed Tomography (CT) scans for the diagnosis and clinical management prior to the pathological examination. It is because of the contrast enhancement on CT images that can be helpful to distinguish the tumor region from the liver parenchyma. However, recognizing tumor regions is still a challenging task for radiologists due to high inter-class similarity, intra-class variations, and fussy boundaries of the tumors. To address these issues, computer-aided detection system is highly useful to establish diagnostic standards to bridge the cognition gap in all levels of radiological expertise.

There are some challenges still remaining to develop computer-aided automatic liver tumor segmentation solution. The high cost of collecting data to conduct experiments. Data labeling is time-consuming and tedious task to prepare proper medical dataset to train and test the model. Another major issue that causes the misclassification of tumor regions is tumor diversity. Tumor can appear in different shapes at different locations with

[1]Perceptual Intelligent Computing Laboratory, Department of Computer Engineering, Faculty of Engineering, Chulalongkorn University, Bangkok 10330, Thailand. [2]Eikonnex AI Co., Ltd., Bangkok, Thailand. [3]Department of Radiology, Faculty of Medicine, Chulalongkorn University, Bangkok 10330, Thailand. [4]Applied Digital Technology in Medicine (ATM) Research Group, Faculty of Engineering, Chulalongkorn University, Bangkok 10330, Thailand. ✉email: thanarat.c@chula.ac.th

Thank You!